Optimal design of spacers in reverse osmosis

Haidari, A. H.; Heijman, S. G.J.; van der Meer, W. G.J.

DOI
10.1016/j.seppur.2017.10.042

Publication date
2018

Document Version
Final published version

Published in
Separation and Purification Technology

Separation and Purification Technology 192 (2018) 441–456

Contents lists available at ScienceDirect

Separation and Purification Technology

journal homepage: www.elsevier.com/locate/seppur

Review

Optimal design of spacers in reverse osmosis

A.H. Haidari[a,*], S.G.J. Heijman[a], W.G.J. van der Meer[a,b,c]

[a] Delft University of Technology, Department of Civil Engineering, Stevinweg 01, 2628 CN Delft, The Netherlands
[b] Oasen, P.O. Box 122, 2800 AC Gouda, the Netherlands
[c] University of Twente, Faculty of Science and Technology, Drienerlolaan 5, 7522 NB Enschede, The Netherlands

ARTICLE INFO

Keywords:
Spacers
Spiral-wound membrane modules
Visualization
Membrane
Reverse osmosis

ABSTRACT

Spiral-wound membrane (SWM) modules are the most common membrane configuration utilized in reverse osmosis (RO) and nanofiltration. The enhancement of SWM module design, particularly in the geometric design of the feed spacer, can play a crucial role in the cost and the potential for wider application of these modules. The feed spacer influences the flux, pressure losses and fouling in the membrane process and consequently the product water unit cost. Despite the shift in the application of SWM modules of RO toward low salinity sources and the resulting higher sensitivity performance using these waters, the configuration and orientation of feed spacers have not significantly changed since the original design. A wider use of SWM modules, therefore, requires the adaptation of geometric parameters of the feed spacer to the water source. Improving the feed spacer's design according to the feed water type requires the knowledge of previous studies conducted in spacer-filled channels as well as further needed investigations in future. This paper reviews the role of the feed spacer in SWM modules and provides an overview of studies conducted in narrow spacer-filled channels to determine the effect of different geometric characteristics of the feed spacer on hydraulic conditions.

1. Introduction

Reverse osmosis (RO) has been used as a desalination technique for more than six decades. Historically, RO-membranes were designed for the production of drinking water by desalination of seawater and brackish water. Currently, RO is a popular technology for the production of highly purified water used in drinking water, dialysis, power generation, pharmaceuticals and medical devices, semiconductor manufacturing, and the paper, sugar, beverage, and horticulture industries as well as in the concentration and reclamation of wastewater [1–10].

Fig. 1 outlines the global NF/RO capacity by feed water (A) and by region (B). Although the use of RO for seawater desalination is still dominating the RO market (Fig. 1A), there has not been a notable increase in the use of RO for seawater desalination compared to RO application for other feed sources since 2002 [12]. In contrast, there has been an increase of about 40% in use of RO for purification of river water compared to the global installed capacity from 2002 [12]. Fig. 1B indicates that RO application for purification of river water happens primarily in parts of the world with rapid industrial growth and strict environmental policy. Given the environmental trends, the application of RO is projected to increase globally in the coming years due to forthcoming environmental regulations in these areas and the influences that these measures would have on other parts around the world.

The spiral-wound membrane (SWM) configuration is predominately applied in NF and RO because they offer a good balance between ease of operation, fouling control, permeation rate, and packing density [13–16]. A wider and a more efficient application of this configuration requires further improvements in different parts of the module. The feed spacer, as an essential part of these modules, has an important role in determining the hydraulic conditions of the feed channel; i.e. pressure drop and cross-flow velocity. The pressure drop is usually associated with the membrane operational cost and the cross-flow velocity with the membrane fouling. Despite numerous studies conducted on the feed spacer in different membrane applications, the modification of the feed spacer in RO has been limited to only a small increase in the thickness of this component.

This paper will review studies conducted to determine the effects that feed spacers have on hydraulic conditions in the spacer-filled channels such as those that encountered in SWM modules of RO. First, this review provides a general background about SWM module configuration and related improvements and geometric characterizations of the feed spacer in particular. Next, it gives an overview of how feed spacers affect the efficiency and productivity performance of SWM modules with respect to the membrane production, pressure drop, and

* Corresponding author at: Room S03.02.20, Stevinweg 03 (Building 23 = Civil Engineering faculty of Delft university of technology), 2628CN Delft, The Netherlands.
E-mail address: a.h.haidari@tudelft.nl (A.H. Haidari).

http://dx.doi.org/10.1016/j.seppur.2017.10.042
Received 26 July 2017; Accepted 17 October 2017
Available online 23 October 2017

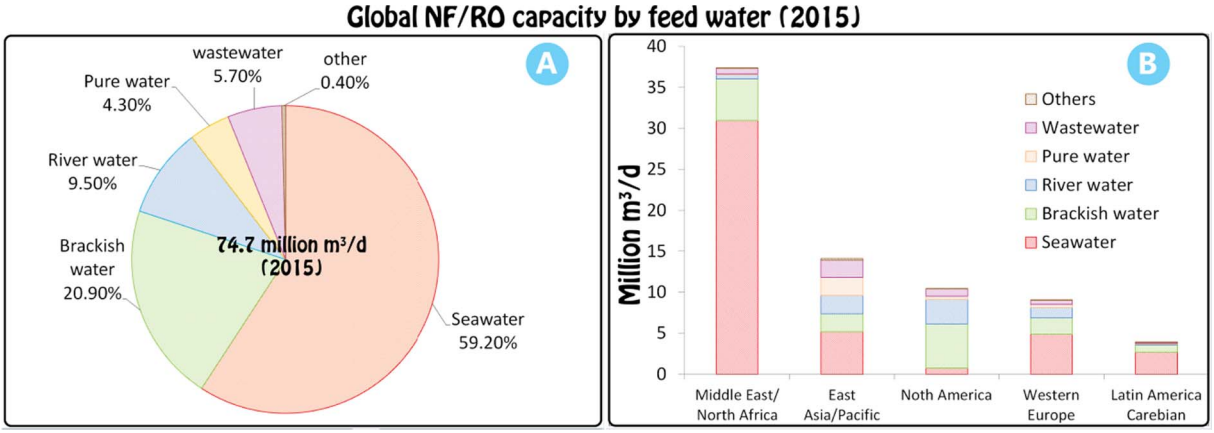

Fig. 1. Global installed NF/RO capacity by feed water (A) and by region (B). The raw data obtained from DesalData [11].

fouling. Finally, it discusses effects of the spacer geometry on hydraulic conditions of the feed channel. The main aim of this paper is to provide the reader with an overview about the areas investigated and those that still need attention for feed spacer design in RO. This overview can also be used for other spacer-related membrane technologies working with nonwoven spacers.

2. Background

Each SWM module of RO (Fig. 2) consists of envelopes, a permeate tube, permeate spacers and feed spacers [17].

The permeate spacer is inside the envelope and creates a flow pass for permeate water. Additionally, it supports the membrane sheets mechanically against (high) feed pressure [18], and therefore it is made of woven spacers with low permeability to have the required stiffness. This low permeability can have great impact on the pressure drop. However, the pressure drop in the permeate channel of RO is usually neglected by manufactures because SWM modules are historically designed for application in the seawater desalination. Schock and Miquel [19] reported that contrary to manufacturers' claims, the pressure losses in the permeate channel are not negligible. Koutsou et al. [20] confirmed the importance of pressure drop in permeate channel especially for the membrane modules applied on low salinity water. Additionally, they [20] mentioned that stiff and incompressible construction of the permeate spacer is of importance for seawater desalination due to high applied pressure in these modules. The feed spacer, which is more porous, lies between two envelopes in a way that it faces the active layer of each envelope. The feed spacer works as a supporting net and keeps the two adjacent envelopes apart [21,22]; thereby, it provides a passing channel for feed water to move tangentially over the active layer of the membrane [23].

Cost savings in RO would make this technology widely available for sustainable and affordable water production in every corner of the globe. An effective method to achieve this target is to improve the SWM modules because the SWM module is the most applied configuration in RO. These improvements include transformation and consolidation in membrane sheet chemistry, re-evaluation of the module design, and optimization of the RO-plant configuration and operation [24]. Among the aforementioned improvements, the impact of module design is most significant. Table 1 provides an overview of some improvements regarding the module design of SWM of RO.

As mentioned in Table 1, investigations of the optimal number of envelopes in a module [19–21] agree that the optimal SWM module design can be achieved with the highest number of envelopes when glue-line effects are neglected. It is important to consider the width of the glue-line in determining the optimal number of envelopes because for a higher number of envelopes, it reduces the membrane active area. The optimal number of envelopes in an SWM module of RO including the glue-line has only been determined by the practical work of Schock and Miquel [19]. Using a 4-in membrane, Schock and Miguel found that by increasing the width of glue-line, the optimal module design is at a lower number of envelopes. They [19] found an optimal of 4–6 envelopes for a 4-in module with a glue-line width of 40 mm and optimal of 3–4 envelopes for the same module diameter and a glue line of

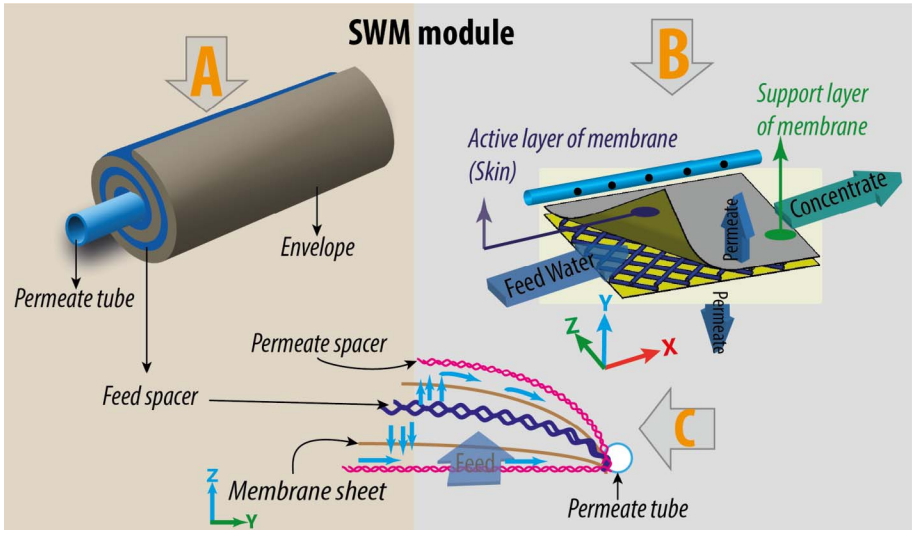

Fig. 2. A schematic view of SWM module out of the pressure vessel (A), unwrapped situation with only two envelopes (B) and side view of the feed channel (C).

Table 1
Selected studies addressing geometric improvements made in SWM modules.

Improvement		Results	Ref.
Module design	Using pressure vessels with two lead elements	The shear will be reduced. This results in formation of a more fluffy biofilm. A fluffy biofilm can be removed more easily with mechanical cleaning than impacted biofilm	[25,26]
	Reducing the number of elements in a pressure vessel	Linear velocity will be reduced and consequently the pressure losses. This results in productivity enhancement of a module. The impact of biomass was reduced on module performance	[25,26] [27]
	Diameter of a module	The increase in the membrane diameter results in the reduction of costs due to a reduction of the system footprint, numbers of housing, piping interconnection and seals between the modules	[28,29]
	Length of a module	An element should be as large as possible to obtain maximal production yet small enough to be handled and installed by a single individual The standard element length is one meter because the industry has commonly made membrane sheets with a width of approximately one meter	[30]
Envelope	Number of envelopes in a module	The optimal numbers of the leaves are almost independent of the concentration, permeability of the membrane, transmembrane pressure (TMP) difference, and thickness of the feed and permeate spacers	[19,21]
		The optimal geometry of the SWM module is reached at the highest number of membrane envelopes, when the glue-line is not considered	[19–21]
	Width of envelope	For a constant membrane area, the highest optimal design is when the width of the envelope is the smallest	[20]
Permeate spacer	Thickness	0.2–0.4 mm	[19]
	Configuration	Woven	
	Pressure losses	Contrary to claims of manufacturers, the pressure losses in permeate channel are not negligible	[19]
Feed spacer	Increasing the feed spacer thickness from 0.7 mm to 0.86 mm	0.86 mm thick spacer had a lower fouling tendency, cleaning frequency, and pressure drop	[31]

80 mm. Manufactures normally produce 4-in SWM modules with 6–8 envelopes. Koutsou et al. [20] and van der Meer et al. [21] referred to the importance of the glue-line but they did not mentioned the optimal number of envelopes including the glue-line.

To the authors' knowledge, Koutosu et al. [20] conducted the only study of the effect of membrane width on module performance. They found [20] that given a constant membrane area (37 m^2 for 8–in membrane), when the width of membrane decrease to its half, the number of envelopes increases, which results in module performance enhancement due to more uniform spatial distribution of the trans membrane pressure. In this study [20], the effect of the glue-line was neglected, which affects the productivity of the membrane. Additionally, it was not mentioned how the increase in the number of envelopes would affect the feed and permeate flow, particularly in the area adjacent to the permeate tube.

Table 1 also shows that a slight increase in the feed spacer thickness causes a lower fouling tendency, cleaning frequency, and pressure drop in the membrane modules. However, the extent of the effect of spacer thickness increase on different factors is not exactly clear from the study because the spacer was chemically enhanced by biocides on top of its thickness enlargement.

2.1. Membrane productivity

Arguably, one of the greatest improvements in the SWM module of RO took place when cellulose acetate membrane sheets were replaced with a polyamide and composite configuration. This transformation led to an increase in the productivity of and rejection by SWM modules of RO. For instance, it is reported [24,32,33] that compared to 8-in cellulose acetate membranes, the capacity of 8-in seawater RO elements made of a polyamide and composite configuration is doubled and the salt passage is decreased about threefold. The cost of water produced by RO is calculated using ratio of operational and capital expenses to the production capacity. The product unit cost decreases with the increase of production volume at a given set of operating parameters. The production capacity is related to the average permeate flux defined as the flow rate of permeate per unit of membrane area (Eq. (1)).

$$J_{ave} = \frac{Q_p}{A_{mem}} = NDP \times K_w \text{(depends on the temperature)} \quad (1)$$

The membrane permeability for water (K_w), which is also known as the mass transfer coefficient of the membrane for water or the specific flux (J_{SPE}), depends on the temperature (Eq. (2)).

$$K_w = J_{SPE} = \frac{J_{ave} \times TCF}{NDP} \quad (2)$$

TCF in Eq. (2) refers to the temperature correction factor and depends on the choice of reference temperature. Commonly, a reference temperature of 25 °C is used as the reference to match the current literature on membrane filtration and the standard test conditions for the membranes as specified by the membrane suppliers. The reference temperature can be based on the local parameters and conditions. For instance, a reference temperature of 10 °C is used in some countries and for some specific applications.

At a given set of operating parameters, the average permeate flux determines the size of RO train and number of elements required, therefore influencing the capital expenses. The average permeate flux at a constant temperature is determined using two known parameters: the membrane permeability (K_W) and net driving pressure (NDP). Treatment plants typically work at a constant production rate; i.e. a higher membrane permeability (mass transfer coefficient) results in a lower and required feed pressure.

In addition to the NDP and temperature, modifying the membrane sheet or increasing the shear at the boundary layers can increase the membrane permeability. The membrane sheet allows the transport of some compounds and prevent or delay the transportation of others and can have a symmetric or asymmetric configuration [8,9,34–41]. The first asymmetric RO membranes produced by Loeb and Sourirajan [42] were made of cellulose acetate and showed up to 100 times higher flux than any symmetric membranes known. The composite configuration of a membrane is made of a fragile discriminating layer with high selectivity (active layer) affixed to a porous support layer (non-active layer) [43,44]. The support layer protects the ripping or breaking of the membrane sheet, while the active layer is responsible for the mass transport and the membrane selectivity.

2.1.1. Productivity reduction

At a constant NDP, the average permeate flux decreases over time because of the degradation of specific permeate flux (membrane permeability) due to fouling formation [3,45]; i.e. fouling results in decreased production capacity when a system operates at a constant NDP. The fouling rate is a function of the permeate flux rate relative to the

crossflow rate. A higher average permeate flux causes a higher concentration of particles at the membrane surface and a higher fouling formation rate. Therefore, fouling reduces the average permeate flux and increases the pressure drop of the membrane [46,47]. The primary fouling mechanisms in RO are related to deposition of inorganic, colloidal and organic materials as well as microorganisms [48] in the feed channel either on the membrane surface or on the feed spacer. The extent and nature of fouling is related to several factors such as feed solution properties (concentration, pH, ionic strength, and component interactions), the membrane module configuration, membrane sheet characteristics (hydrophobicity, charge, roughness, pore size, pore size distribution and porosity), and operating conditions (temperature, NDP and cross-flow velocity).

In addition to fouling, concentration polarization is another serious concern in the production capacity reduction of a membrane system. Concentration polarization is the consequence of water permeation, causing a higher salt concentration directly adjacent to the membrane sheets compared to the bulk of fluid. Thus, concentration polarization is not a fouling type, but it reduces the membrane productivity by lowering the permeation of water through the membrane and enhancing the fouling formation [3,45,49] on the membrane. For instance, scaling is a consequence of the salt concentration increase as the sparingly soluble salts reach their solubility limit and deposit on the membrane surface [50,51]. As with the fouling, the degree of concentration polarization depends on the ratio of the permeate flow rate to cross-flow, with greater concentration polarization resulting from a higher permeate flow. This is the reason that concentration polarization is worse in the composite membranes, which have a higher permeate flow at the same pressure compared to cellulose acetate and polyamide membranes.

Among different types of fouling, biofouling is probably the most difficult type to control because of the complexity of the ecosystems causing it [27,52–58]. Biofouling is defined as a structured community of bacterial cells adhering to an inert or living surface due to attachment and growth [59–63]. The degree of biofouling is usually determined by measurement of ATP (adenosine triphosphate) for total living biomass [64] and TOC (total organic carbon) for total accumulated biomass [65,66]. Biofouling can occur with a minimal number of microbial cells that adsorb to a surface and create a conditioning layer for more biomass accumulation [67,68].

In SWM modules, spacers are regarded as the starting point for biofouling. The biofilm growth favors the feed spacer's junctions close to the module inlet, which leads to a distortion of the flow field and the creation of regions with low-velocity values close to the spacers' intersections [69]. With time, the biofilm accumulates further, eventually clogging a part of the feed channel and spreading the stagnant regions. As a result, the fluid stream through the flow channels is hindered, preferential channels are formed, and consequently, the permeate flow decreases [69–71].

2.1.2. Productivity improvement

Effective fouling control to improve the membrane productivity is possible by having sufficient information about the feed water and a profound understanding of fouling mechanisms and hydrodynamic conditions inside the feed channel. However, the fouling mechanisms are often complex and become even more complicated knowing that a remediation method for one type of fouling mechanism could worsen other types. For instance, increasing the axial flow rate is an effective way of removing the colloidal matter from the membrane surface and reducing the fluid resistance close to the membrane surface (reducing the thickness of concentration polarization layer) due to better flow mixing [72–74], but it is not effective in removal of biofouling. On one hand, the higher flow rate leads to a higher transport of nutrient into the flow cell and higher biomass formation; on the other, the biofilm formed at a higher rate of axial flow is more compact and harder to remove compared to the fluffy biofilm formed at lower shear [71,75–86]. Consequently, given our current knowledge, total fouling prevention seems to be impossible, and using a single curative method to combat all fouling types is not practical.

Operating the system at a higher shear than operational shear is generally considered an effective way of reducing the fouling and increasing the average permeate flux. A higher shear can be achieved by increasing the axial flow rate, creating flow instabilities, applying two-phase flow, and using a feed spacer. Rotation of the membrane [87] and flow pulsating [88,89] are possible techniques to make the flow unstable. However, these techniques are (i) expensive and (ii) not always easy to apply in SWM modules of RO. Application of a higher axial flow rate as the only method to increase the shear is not economically attractive because the required mixing in the flow, which is needed to effectively decrease the thickness of boundary layer, causes a high pressure drop. Using rotational shear and two-phase flow in addition to the increase of normal axial shear is suggested to be more effective in fouling removal [45,73]. For example, the rotational shear can be generated by using double inlet/outlet flow cells. Kim et al. [90] and Balster et al. [91] examined the effect of rotational flow on the average permeate flux. These studies [90,91] found that rotational flow has only a marginal effect on the flux enhancement. The impact of air sparging (two-phase flow) on the improvement of mass transfer was a function of the air/water ratio, bubble size, air distribution patterns, and duration of the air sparging [91–97]. Table 2 shows some investigation on the mechanisms of mass transfer enhancement.

Periodic membrane cleaning with chemicals and dosing of chemicals in pretreatment are common methods to prevent and control membrane fouling [54,100–104]. The chemical cleaning, however, is (i) expensive, (ii) of environmental concerns (discharge regulations), (iii) not always effective, and (iv) a danger to the membrane lifespan. The price of scale inhibitors and cleaning chemicals alone is reported to be around 5–25% of operational costs [51].

Biofouling control is of particular importance in SWM modules of RO, especially when wastewater, seawater, and fresh surface water are used as the feed. Presently, chemical cleaning is one of the most widely

Table 2
Selected studies conducted on mass transfer enhancement.

Technique	Specification	Field	Effect of modification on mass transfer	Ref.
Multi-layer spacer	3-layer spacer	UF	More turbulence and therefore less fouling and a higher mass transfer was observed	[98]
		ED	20% higher mass transfer compared with two 2-layer	[99]
Two-phase flow	Empty channel	ED	With the increase of the gas to liquid ratio from 0 to 0.9, 70% increase in mass transfer was observed	[91]
	Single-layer net-type spacer		With the increase of the gas to liquid ratio from 0 to 0.9, 50% increase in mass transfer was observed	
	Multi-layer spacer		With the increase of the gas to liquid ratio from 0 to 0.9, no significant increase in mass transfer is observed	
	Using baffles	MBR	A better distribution of bubbles and the size of bubbles Could be used to lower the fouling and enhance the mass transfer	[94]
Double inlet/outlet cell	Empty feed channel	ED	The mass transfer was the same as single inlet/outlet channel	[91]
	Single layer-net-type spacer		Improvement was less compared to single inlet/outlet channel	
	Multi-layer spacer		Improvement was insignificant compared to single inlet/outlet channel	

employed techniques for inactivating and removing biomass from RO and NF [102]. This method normally involves dosing biocidal chemicals in the feed water of a membrane system in order to destroy the biofilms [100,101]. Several biocidal chemical agents have been documented for this use, ranging from acidic cleaning to caustic cleaning and enzymatic cleaning techniques [102,103]. Multiple studies have shown that a very low dosage of copper [85,105] and other metals such as silver and gold could be efficient in disinfecting water against microbial biofilms. However, chemical agents are known to reduce the lifespan of the membranes [100]. Additionally, biofilms have a high degree of resistance to many disinfectants, even against antimicrobial compounds such as metal ions [104]. Finally, chemical cleaning could be ineffective due to the effect that it has on other non-targeted fouling types or due to the effect that traces of chemical cleaning has on other locations in the treatment plant. For instance, ineffectiveness of chemical cleaning could be due to residues leakage of chemicals from pretreatment to membrane unit. In this context, it has been shown that systems with continuous chlorination have a higher rate of membrane biofouling [106–108]. This is most likely due to the formation of assimilable organic carbon (AOC), which serves as indicator of the biological stability of the water, with high levels leading to the biological (re)growth during subsequent return to normal water production through the particulate fouling [61,70]. Table 3 provides a short overview of biofouling control studies.

2.2. Energy and pressure drop

Studies have shown that energy is a major contributor to the operational costs of RO systems. The required energy for an RO system includes the energy for pumping the feed water, running equipment during pre- and post-treatment and operating the transfer pumps and high-pressure pumps, among which feed pressure pumps require the most energy to operate [120–122]. The power consumption of a feed pump is a function of feed pressure, recovery and equipment efficiency. At a determined feed pressure, the average flux (J_{ave}) over a module decreases because NDP (Eq. (3)) decreases as a result of the increase in flow friction losses and osmotic pressure of the feed [120].

$$NDP = \frac{J_{ave}}{K_W} = P_{TMP} - \pi_{TMP} = (P_f - P_P) - (\pi_f - \pi_P) = \left(\frac{P_F + P_C}{2} - P_P\right) - \left(\frac{\pi_F + \pi_C}{2} - \pi_P\right) \quad (3)$$

NDP is a measure of available driving pressure to force the water through the membrane from the feed side to the permeate side and is related to the average permeate flux of the system (J_{ave}) and membrane permeability (K_W) [120,123]. The available driving pressure is the difference of the transmembrane pressure and transmembrane osmotic pressure.

The pressure losses could be expressed in terms of total pressure drop (ΔP), which is the sum of the pressure drops at successive pressure vessels, interconnections of membrane elements, the permeate channel and the feed channel. The pressure drop in the sequential pressure

Table 3
Selected studies addressing methods for biofouling control.

Method	Suggested mechanism	Effectiveness	Literature
Copper dosage	Copper is thought to be cytotoxic by causing changes in the plasma membrane permeability or efflux of intracellular K^+ during the entry of Cu^{2+} ions	A reduction of biomass concentration (8000 pg ATP/cm2) and pressure drop (18%) with a daily dosage of copper sulfate was achieved	[70]
	Copper can participate in Fenton-like reactions, generating reactive hydroxyl radicals, which can cause cellular damage imparted via oxidative stress		[109]
	Copper is believed to interfere with enzymes involved in cellular respiration and bind to DNA at specific sites		[110]
	Adding copper to water causes a reduction of the contact angle and hence an increase in the hydrophobicity of the feed spacer, which results in a decreased likelihood of biofouling		[104]
Nutrient loading	Nutrient loading is a function of substrate concentration and the linear flow velocity	For a limited substrate load, microorganisms attune themselves to the environment by changing their morphology	[86,111]
Linear velocity	Limiting linear velocity causes less nutrient loading and therefore a lower probability of biofouling	The formed biofilms were more compact and harder to remove	[71,86,112]
Gas sparging	Gas sparging causes an increase of shear It is a function of air to water ratio, bubble size, air distribution patterns and duration of the sparging	Less effective in SWM of RO than MF and UF	[113,114] [91–97]
		The formed biofilms were more compact and harder to remove	[75,77,79,81,82,86,115]
		Complete removal of biofilm was not achieved. The remaining bacteria on the spacer/ membrane caused a rapid regrowth and accumulation of cells	[116]
		Fouling attributed to inhomogeneous air distribution and channeling of the airflow, which can cause incomplete cleaning and an enhancement of scaling.	[93,95,96,117]
Feed flow reversal	The feed flow reversal results in re-dissolution of the deposited scale into the solution	The feed flow reversal reduces the impact of biomass on membrane performance and gradually decreases the amount of biomass over time	[7,27]
CO_2 nucleation	Nucleation within the flow channel is due to local pressure differences as well as the presence of rough spots as the nucleation sites. Upon their formation, the bubbles are swept along with the flow due to their coalescing with larger bubbles, and the flow channel will become clean.	Efficiency of this method is higher than air/water cleaning due to that no stagnant bubbles or bubble channeling is formed	[118]
	Rough spots (junctions and filaments of spacers) enhanced the nucleation and subsequent growth of the bubbles	A higher removal efficiency is achieved compared to the air/water cleaning	[118,119]

vessels and successive modules in a pressure vessel can be minimized with an optimal design of the pipes and interconnectors. In an SWM module, usually only the pressure drop in the feed channel (Δp) accounts for the pressure drop calculation. Permeate pressure drop has been shown [19] to have potentially more than minor effects on the total pressure losses. Effects of permeate pressure losses on the feed pressure become particularly important in low salinity water sources, but there is a limited number of investigations in this area.

The feed channel pressure drop includes frictions as a consequence of the (clean) channel geometry and frictions as a consequence of fouling. The clean feed channel pressure drop is a function of frictions at the walls and the feed spacer as well as changes in flow directions and flow patterns. Generally, the presence of the feed spacer has greater effects on the pressure drop than the channel walls [124,125].

3. Optimal feed spacers

An optimal membrane module is one with the highest production rate at the lowest energy consumption and expense possible. One approach towards the design of such an SWM module is to optimize the feed spacer geometry. Theoretically, an ideal feed spacer is defined as a spacer with the perfect hydrodynamic design [126], i.e. a spacer that neither causes stagnant regions nor blocks the membrane surface area [127]. Stagnant areas cause solids and/or microorganisms to accumulate and/or rejected salts to build up [126,127], and the resulting smaller membrane surface results in a reduced production rate. In practice, an optimal feed spacer is defined as a design that achieves a balance between competing concerns: the mass transfer on one hand and the pressure drop and fouling on the other. For instance, using a feed spacer in an empty channel causes a mass transfer enhancement [13,15,19,23,124,126–132] but at the expense of increased pressure losses along the feed channel [14,15,19,23,124,126,128,129,132–134]. Additionally, the use of a feed spacer in an empty channel reduces effects of concentration polarization but at the expense of the formation of stagnant regions, which are favorable for particle deposition and biomass formation, either downstream [86] or upstream [135] of a spacer. It is reported that feed spacers have a higher impact on the pressure drop (2.5–160 times compared to an empty channel) than flux enhancement (2–5 times) [129,136]. Therefore, the optimal feed spacer is the one that results in a flux improvement without a (significant) increase in pressure losses. It is typically more economically attractive to operate membrane systems with a spacer than without because the benefits of mass transfer often outweigh the disadvantages caused by increased energy losses. Therefore, the main reason for using a feed spacer in SWM modules of RO is to enhance the mass transfer, which is often described by the diffusion model. According to this model, average water flux (J_{ave}) through the membrane is a function of applied pressure over the membrane sheet (NDP), the membrane mass transfer coefficient (K_w) or specific permeate flux (J_{SPE}) and temperature (TCF) (Eq. (2): $K_W = J_{ave} * TCF/NDP$). The Sherwood number (Eq. (4)), which incorporates the effect of the Reynolds number (*Re*) and Schmidt number (*Sc*), is commonly used to predict the membrane mass transfer coefficient (K_w).

$$Sh = K_w \times Re^a \times Sc^b \times \left(\frac{Z \cdot d_h}{L}\right)^c \tag{4}$$

The Sherwood number depends on several constants. Table 4 shows the common values used for the constants of Sherwood numbers for the empty and spacer-filled channels. Spacer-filled channels with zigzag spacers (diamond shape) are considered to be channels in which the flow direction is changed. Channels with ladder type or cavity type spacers are usually considered to be channels without changes in flow direction, containing one set of filaments parallel to flow and other set perpendicular to flow direction.

The last term of the Sherwood number can be neglected in the empty rectangular channels because the constant "Z" is equal to zero in the empty feed channel. The constant "a" for the spacer-filled channel is reported to be around 0.5. Da Costa et al. [129] found values range from 0.49 to 0.66, Kurada et al. [137] mentioned a value of 0.5, and Schwager et al. [138] reported 0.62.

Table 4
Constants for the calculation of Sherwood number for empty rectangular-shaped channels and spacer-filled channels.

Type of the feed channel	K_W	a	b	c	Z	Error	Ref.
Empty rectangular feed channel	0.66	−1/2	−2/3	0	0	–	
Spacer filled channel without changes in flow direction	0.664	1/2	1/3	1/2	1	30%	[124]
Spacer filled channel with changes in flow direction	$0.664k_{dc}$	1/2	1/3	1/2	2	10%	[124]

Da Costa et al. [124] investigated the mass transfer coefficient achieved for spacer-filled channels using Eq. (4) and the constants mentioned in Table 4 and found that the mass transfer coefficient differs 30% from the practical value for spacers that do not change the flow direction and 10% for spacers that change the flow direction. In zigzag spacers, which are commonly used in SWM modules, the constant K is related to factor k_{dc}, which is a function of geometrical characteristics of the spacer such as the ratio of filament thickness to the channel height (d/H_{CH}), porosity (ε) and hydrodynamic angle (α) (Fig. 5) [124,139].

The relationship between the pressure losses and the flow through the channel can be described by determining flow characteristics. However, because the flow characteristics of a spacer-filled channel are too complicated, the friction factor and the pressure drop dependency on the velocity are used to elucidate this relation. The friction factor (C_{td} in Eq. (5)) is defined in terms of three components: the kinetic energy per unit volume of feed, pressure drop per unit length of the flow path and characteristic dimensions of the channel.

$$C_{td} = \frac{2}{\rho \cdot u_{ave}^2} \cdot \frac{dp}{L} \cdot d_h = \frac{A'b}{Re^n} \tag{5}$$

Eq. (5) is a semi-empirical equation, which means that the pressure drop over the membrane has to be measured in order to determine the friction factor. The friction factor in Eq. (5) is typically expressed as a function of the Reynolds number to a specific power (Re^n) and channel geometry (A′). In the case of an empty rectangular channel, a value of 24 can be assigned to A′ [124,140]. The Reynolds number is a function of inertial and viscous force.

$$Re = u_{ave} \cdot d_H \cdot \frac{\rho}{\mu} \tag{6}$$

The viscous forces are often kept constant in membrane filtration experiments and the inertial forces are a function of the hydraulic diameter, flow density and viscosity. The initial increase of the Reynolds number during steady flow causes slight oscillations, which are superimposed on the steady flow pattern, and flow instabilities appear as a result. A further increase of the Reynolds number causes an increase in the amplitude of the oscillations, which gives rise to flow with considerable mixing [141]. Table 5 outlines studies that investigate the effect of the Reynolds number on the hydraulic conditions of the feed channel.

The hydraulic diameter (d_H) is used to correlate the flow through non-circular or complex channels with a constant cross-sectional area, i.e. hydraulic diameter serves as the characteristic channel dimension [19,97,124,145,146]. Attempts to relate the hydraulic diameter to the flow behavior by a single equation in the spacer-filled channel had only limited success [145].

$$d_H = \frac{4 \times \varepsilon}{\frac{2}{H_{CH}} + (1-\varepsilon) S_{v,SP}} \tag{7}$$

Table 5
The effect of *Re* on different parameters.

Spacer/process	*Re*	Effect	Ref.
Net-type spacers	50	The flow was in an average direction	[141]
	35–45	Numerical study shows that transition to unsteady flow occurs at relatively low Reynolds numbers; i.e. *Re* = 35–45	[142]
	30	The experimental studies with particle image velocimetry (PIV) shows that unsteady flow for common feed spacer	This thesis
	180–280	Most geometries started to exhibit oscillations	[141]
	250–300	Flow became unsteady and wavy	
	> 300	Flow showed a very unsteady behavior	
	$10 < Re < 100$	Flow separation and boundary layer development play a role in mass transfer enhancement	[143] [99]
	Re > 100	Longitudinal and transversal swirling causes mass transfer enhancement due to mixing	[99]
Compared strip-type shaped promoter or eddy promoters with net-type spacer in electrodialysis		Compared to the strip-type promoters, the net-type promoters were more efficient at the lower Reynolds numbers	[144]
	Re > 400	Sherwood number of net-type mesh became equal to or slightly smaller than that of the strip-type promoters, likely because the eddy generation mechanism in the net-type spacer is affected by the flow attack angle	

The hydraulic diameter depends on the channel height (H_{CH}), spacer porosity (ε), and specific surface of the spacer ($S_{v,sp}$). Eq. (8) provides a formula for estimation of the spacer porosity (ε). In this formula, the porosity is estimated with the channel height or spacer thickness, orientation of longitudinal and transverse filaments with respect to each other and the filaments' geometry.

$$\varepsilon = 1-\frac{V_{sp}}{V_{mesh}} = 1-\left(\frac{A_{CT}\cdot lm_{CT} + A_{CP}\cdot lm_{CP}}{lm_{CT} * lm_{CP} * \sin(\beta) * H_{CH}}\right) \quad (8)$$

Eq. (9) is a simplified form of Eq. (8) for the feed spacers of SWM modules of RO in which the top and bottom filaments have the same average diameter and mesh length.

$$\varepsilon = 1-\frac{\pi\cdot d}{4\cdot lm\cdot\sin(\beta)} \quad (9)$$

Eq. (10) represents the specific surface of the spacer ($S_{v,sp}$), which depends on the filaments' geometry.

$$S_{V,SP} = \frac{A_{SP}}{V_{SP}} = \frac{P_{CT}\cdot lm_{CT} + P_{CP}\cdot lm_{CP}}{A_{CT}\cdot lm_{CT} + A_{CP}\cdot lm_{CP}} \quad (10)$$

The average inlet velocity in the spacer-filled channel (U_{ave}) is a function of average feed flow (Q_{ave}) and cross-sectional area of the feed channel (A), which depends on the spacer porosity.

$$U_{ave} = \frac{Q_{ave}}{A} = \frac{Q_{ave}}{W\cdot H\cdot\varepsilon} \quad (11)$$

The actual velocity in the spacer-filled channel should be measured at fully developed flow. The flow becomes fully developed after the entrance length, which is about 2.17 cm for a rectangular empty channel with a ratio of 1/50 of channel height to width (H_{CH}/W) [147]. In a spacer-filled channel with ladder spacers, the flow pattern became periodic typically after three to five transversal filaments [148,149].

As previously mentioned, the flow through a spacer-filled channel cannot be described easily like the flow through an empty channel, and therefore Eq. (5) and/or Eq. (12) is used for a better understanding of the flow regime.

$$dp \propto K \times u_{ave}^{m} \quad (12)$$

Eq. (12) describes how the pressure drop is correlated with the volumetric flow rate. It was believed [145,150] that the exponent "m" in Eq. (12) reveals the degree of turbulence in the feed channel. An m-value equal to one was the indication for the laminar flow, a value of 1.75 was the sign for a fully developed turbulent flow and all exponents between these two values were indicators for a transitional regime [145,150]. However, as mentioned in some studies [126,151–154], referring to the flow regimes encountered in SWM modules as "turbulent" is a common misunderstanding because turbulent flow is defined for $Re > 3000$, at which turbulence can be assumed to be isotropic and fully developed while the *Re* in SWM modules of RO remains in the laminar flow regimes ($Re < 300$).

3.1. Investigation of the feed spacer effect

The desire to enhance the performance of RO together with the development history of these membranes encouraged a vast amount of study related to the role of the feed spacer in determining the hydraulic conditions inside the feed channel of SWM modules. Early studies led to a good understanding of the mechanisms that give rise to concentration polarization, and the recent studies have led to a partial understanding of biofouling mechanisms. The role of the feed spacer in SWM modules of RO has been derived from the function of feed spacers in other fields such as in electrodialysis [90,126,155,156], tubular reverse osmosis [157], electrochemical cells [90,91,99,127,136,157–159] and micro- and ultrafiltration processes [15,124,128,129,133,157,160]. In fact, the feed spacers or the flow promoters first became important for membrane mass transport in electrodialysis plants [14,141]. Most electrodialysis studies are performed in flat flow cells and flat sheet membranes. The working mechanisms and principles of flat flow cells and flat sheet membranes are the same as for an unrolled SWM module, and therefore, flat flow cells are commonly used to study the hydraulic conditions in spacer-filled channels of SWM modules [19,161]. The curvature effects of SWM modules on the flow can be neglected because the heights of feed channels in SWM modules are small enough compared to the channel width [149,162]. Flat flow cells provide a simple but effective method for studying flux, pressure drop, fouling and flow pattern visualization in feed channels [15,124,126,129,163,164] in a shorter time and with lower material expenses compared to a full-scale module. Usually, flow cells with permeate production ability are used for studying the flux and concentration polarization, and cells without permeate production are for studying biofouling because the formation of biofouling is not affected by the permeate production [165]. Additionally, feed water ranging from low to high concentration of inorganic substances is used to investigate concentration polarization and (in)organic fouling, and tap water with sodium acetate or a special ratio of combined sodium acetate, sodium nitrate and sodium phosphate (C:P:N) is used to study the biofouling [47,48,69–71,85,86,116,134,166–168].

Visualization is an important method in determining the fluid condition in SWM modules of RO. In previous studies, the velocity profiles utilized were a rough calculation of the actual velocity profile.

Table 6
Selected experiments conducted on visualization of the flow around feed spacers.

Researcher	Visualization method	Ref.
Da Costa et al.	Injected air bubbles and dye for visualization of flow	[124]
In et al.	Implemented a camera and used ink in water for visualization of laminar flow around the spacers	[171]
Kim et al.	Ink is used as the tracer for visualization of the mass transfer in the 3D net-type promoter in electrodialysis	[90]
Geraldes et al.	An aqueous solution of bromophenol blue is used for the visualization of streams in a ladder-type spacer	[172]
Vrouwenvelder et al.	A solution of potassium permanganate ($KMnO_4$) is used for visualization of the flow in a flow cell	[47]
Schulenburg et al.	Nuclear Magnetic Resonance Imaging (NMRI) is used to show the spatial distribution of the biofilm and mapping of the velocity field	[69]
Creber et al.	NMRI is used to show the effect of different chemicals on cleaning of RO and NF	[166]
Willems et al.	PIV is used to visualize the effects of two-phase flow in spacer-filled channels	[117]

Additionally, interactions between multiple ionic components in the feed solution was neglected in those studies [169]. In more recent studies, the velocity profiles and pressure losses in spacer-filled channels are predicted with numerical models [16,21,135,151,168–177], for which excellent reviews are available [14,152,170]. Computational fluid dynamics (CFD) is a common numerical technique in membrane processes for simulation, visualization and analysis of fluid systems. The main advantages of CFD models over experimental methods are the lower material costs and the higher ability to control specific process parameters, e.g. the inlet feed velocity, feed concentration and temperature [169]. The primary challenge for such models is that there are limited direct experimental studies on the detailed velocity profile with resolution at the range relevant for CFD studies to support them. Table 6 summarizes some visualization studies of the flow pattern in spacer-filled channels.

Experimental methods such as injected dyes and particle depositions [90,146,172] give good results for mapping the velocity profile albeit at much lower resolution than numerical studies. Electrochemical methods [117,173], in which numbers of electrodes are embedded into the channel wall, are more often used for visualization in membrane technology. A disadvantage of electrochemical measurements is that they can only be performed in the absence of the membrane in order to accommodate the electrodes [117]. Particle image velocimetry (PIV) is a non-invasive visualization method that offers reasonable spatial and temporal resolution without the need of limiting electrodes. A detailed description of the technique can be obtained from Raffel [174] and Adrain [175]. In membrane technology, PIV can be used to determine the particle deceleration and dead zones as well as for creating fluid velocity mapping in fouling studies (see Fig. 3). However, despite the advantages of PIV, this method is not commonly applied in SWM modules, and there is only a limited number of studies available [117,125,176] using this technique.

In addition to challenges regarding the verification and validation of numerical studies, it is difficult to match the geometry of feed spacers used in most CFD studies with the geometry provided by manufacturer, e.g. intricate characteristics such as the torsion and protrusion between two nodes are difficult to generate. Also, simulation of fouling is a time-consuming and challenging job and need its own experts [169].

4. Geometry of feed spacers

Fig. 4 illustrates different feed spacer configurations that are used in the membrane filtration process. Spacer A is the most common configuration used in SWM modules of nanofiltration and reverse osmosis. Other configurations are used in microfiltration, ultrafiltration, electrodialysis, membrane bioreactors, etc.

A feed spacer in SWM modules of RO typically has a net-type shape and is made of polypropylene. The extruded meshes in these spacers have a two-level structure where the cross filaments are welded in a nonwoven way on top of each other and make an inner angle of 90° with each other (β). The feed spacer in RO (Fig. 5) is oriented at an angle of 45° with the flow (the flow attack angle). The top and bottom filaments have almost an equal average diameter. Along each filament in a mesh, the diameter is neither constant nor perfectly round.

In other applications, such as ultrafiltration, the spacer could consist of thinner filaments perpendicular to flow and thicker filaments parallel to flow (Fig. 4B) [31]. Table 7 shows some studies done on the effect of feed spacer configuration in different fields.

4.1. Modified feed spacer material

Feed spacers are manufactured from variety of materials. Feed

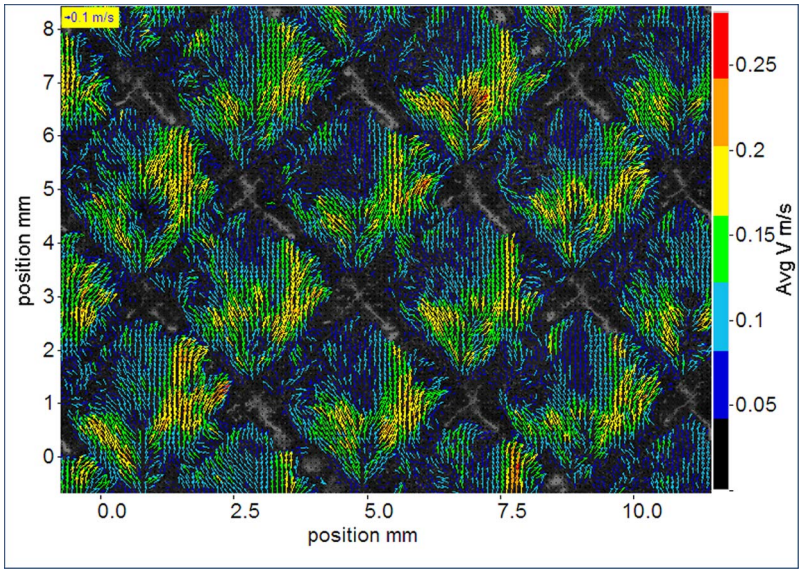

Fig. 3. Fluid velocity mapping measured and created by PIV inside a feed channel of SWM of RO membrane. A clean spacer (28 mils = 0.7 mm) and a clean membrane (Tory AMC1) were used for this experiment. The inflow was about 16 L/h. The average particle diameter was 10 μm. Deceleration of particles occurs close to nodes and spacer filaments, which are also the places that show the highest fouling by autopsy. The highest velocity is found over the filaments and directly downstream of filaments.

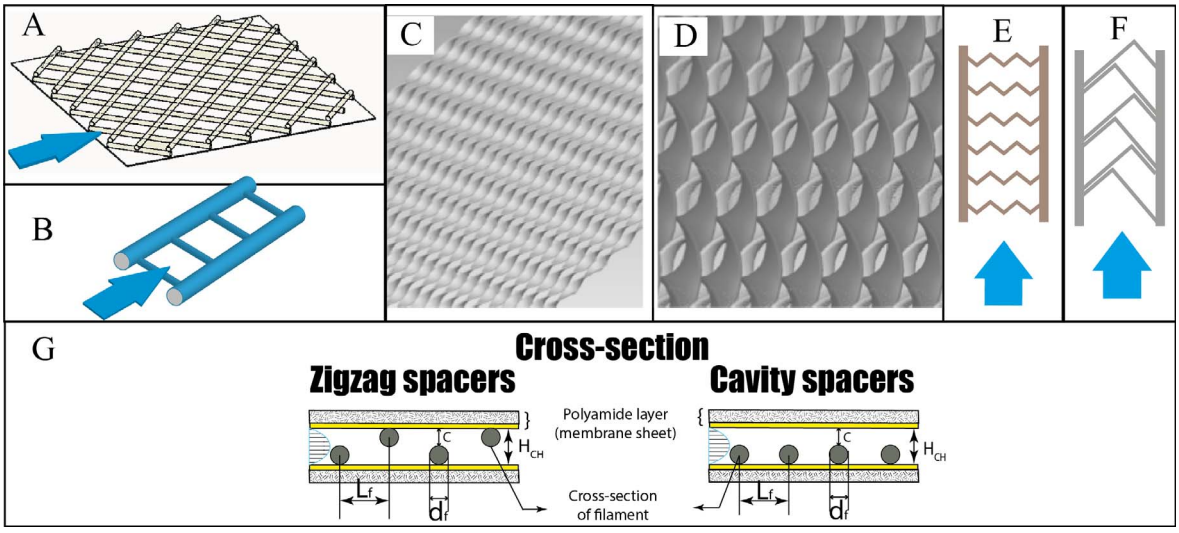

Fig. 4. Typical spacer design; rhombus diamond-type (A), ladder-type (B), monolayer helix (C), double layer helix (D) [143], zigzag-type (Corrugated) (E), herringbones spacer (F). Two possible cross-sections; zigzag-type and cavity-type cross-section (G). The possible geometrical parameters are c/H_{CH}, adaptive height (d_f/H_{CH}), and aspect ratio (L_f/h). L_f is the distance between two filaments, H_{CH} is the channel height, d_f is the average diameter of the filaments and c is the gap between the membrane and the cross filament.

spacers in SWM of RO are made of semi-crystalline thermoplastics such as polypropylene and, to a lesser extent, polyethylene. Feed spacers made of the same material could differ from each other based on the material density, i.e. a polyethylene feed spacer could be low-density polyethylene, polyethylene, or high-density polyethylene. To the authors' knowledge, no investigations have been conducted on the effects that plastic type could have on the pressure drop and fouling of membranes. For instance, it not yet known how the feed spacer stiffness could affect the fouling and different cleaning methods.

Most studies on feed spacer materials used additives to make feed spacers more resistance to biofouling. [19,71,85,105,134]. Most of these studies found that the surface modification to reduce adhesion of microorganisms to the spacer and membrane is not adequate to prevent or limit biofouling [85,105,134]. Additionally, the surface modification did not have a significant impact on the feed channel pressure drop [85,105,134]. Unsuccessful application of modified spacers in biofouling prevention is due to the finding that coated surfaces could only kill microbes under initial conditions, after which a. dead layer of microorganisms will form and cover the antimicrobial coating compounds, preparing the surface for a second layer to be built on top of exposed or even lysed microorganisms.

Araùjo et al. [85] reported that biofouling prevention was not successful with use of a copper-coated feed spacer because the coating agent toxicity became ineffective due to extracellular polymeric substances secreted by microorganisms. This occurs when some microbial strains with a higher resistance to the metal coating first colonize on the coating metal and make the conditions favorable for other microorganisms to accumulate by covering the coated metal with their extracellular polymeric substances. Tsuneda et al. [59] showed that the extracellular polymeric substances are responsible for bacterial adhesion to the solid surface by measuring the polysaccharides using techniques such as FTRI (Fourier transform infrared) spectrometry. Polysaccharides are known to constitute the largest portion of extracellular polymeric substances and are related to cell adhesion during initial stages of biofilm formation [59]. In addition to the ineffectiveness of antimicrobial metals in prevention of biofouling, these antimicrobial metals can potentially leach into the permeate. Moreover, their function in the presence of binding inorganics when applied in full-scale operation has not been investigated.

In addition to the coating of spacers with antimicrobial metal, surface-confined macromolecules known as polymer brushes are also being used to modify the feed spacers. In this technique, the feed spacer surface becomes hydrophilic. Hydrophilic surfaces are known to be resistant to the adhesion of bacteria and proteins [178], i.e. polymer

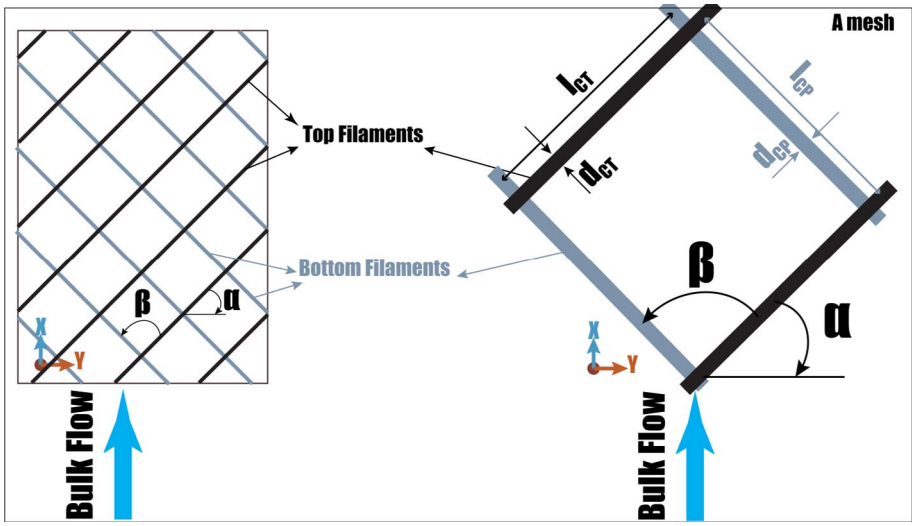

Fig. 5. The extruded meshes in spacers of SWM modules of nanofiltration and reverse osmosis are made of two layers, which are constructed in a nonwoven way.

Table 7
Selected studies comparing different configuration of feed spacers.

Field	Studied configuration	Results	Ref.
ED	Eddy promoter is compared with net-type spacer	The effectiveness of the eddy promoters was only achieved at a high Reynolds number while the efficiency of the net-type promoters was achieved for the whole range of Reynolds numbers	[144]
	Ladder-type spacers with the staggered herringbones	The staggered herringbones were better spacers for enhancing mass transfer The configuration with one herringbone filament provided better enhancement than a group of herringbone filaments because of the complete rotation of the flow	[3]
–	Cavity configuration is compared with zigzag configuration (aspect ratio = 5)	The unsteady flows in the channel begin at a Reynolds number of 250–300 for both spacers used in this study	[171]
UF	Zigzag spacer (Corrugated) is compared with net-type spacer	The pressure drop was lower in the zigzag spacer than the net-type spacer Flux enhancement was a function of feed water properties Zigzag spacers had a better flux enhancement compared to net-type spacer for feed water without fouling	[131]
		The pressure loss and the permeation rate were constant over time for the zigzag spacer, but the net-type spacer showed an increase in the pressure loss over time due to blockage of the spacer mesh	[177]

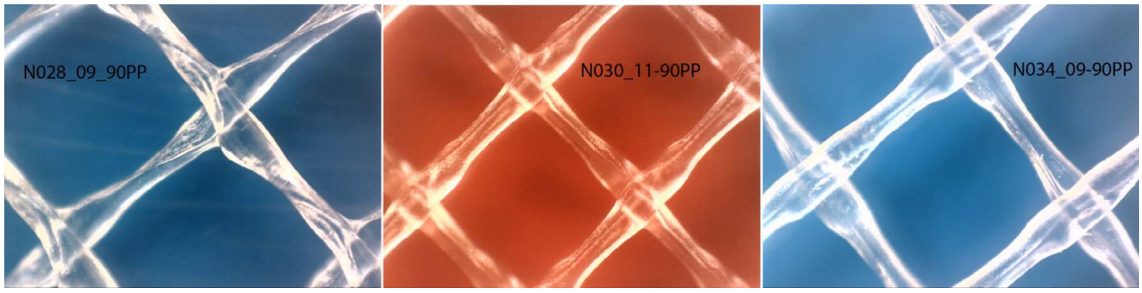

Fig. 6. Three standard spacers used in SWMs of RO with a thickness of 0.71, 0.76 and 0.86 mm respectively from left to right. A turning-liked filament can be observed on the most left spacer but not on the other ones.

brushes reduce the friction between the modified feed spacer and microorganisms and consequently the microbial adhesions [179–181]. Araùjo et al. [85] compared a system containing a biostatic modified feed spacer and membrane with an unmodified system under the same operational conditions. The modified spacer was infused with 0.5 wt% triclosan, an anti-biofouling compound. The results showed the same pressure drop and accumulated biomass in the hydrophilic-modified and unmodified systems [85]. The malfunctioning of the biostatic hydrophilic system was related to rapid leaching of the active compound due to high shear forces, which disrupted the structure of absorbed polymer brush layers and destroyed the complex coacervate-brush structure [182].

4.2. Filament cross-section

Feed spacers are usually composed of filaments with rounded cross-sections. This is the case in spite of results that have shown [183,184] rounded cross-sections are less effective in destabilization of the concentration polarization layer and enhancement of mass transfer compared to other cross-sectional shapes such as a rectangle or triangle. Ahmad et al. [183] found in a CFD-study that spacers with triangular or rectangular cross-sections more effectively destabilize the concentration polarization layer than those with a rounded cross-section. They found that spacers with triangular cross-sections were the most effective spacers for destabilization of the concentration polarization layer. Icoz et al. [184] determined that spacers with hexagonal and square cross-sections enhance heat transfer better than spacers with rounded cross-sections. Amokrane et al. [185] compared the oval and elliptic shaped filaments with rounded filaments and found a higher pressure drop in systems with rounded filaments. Additionally, oval and elliptic cross-sections resulted in a thicker concentration polarization layer and lower mass transfer.

Filaments with rounded cross-section are typically preferred because in contrast to the mass transfer, the pressure drop caused by rounded cross-section filaments is lower than other cross-section shapes [184,186]. The lower pressure drop can be translated into a lower pumping energy, which is one of the primary design considerations for membrane systems. However, due to manufacturing difficulties, the cross-section in an SWM module of RO is not uniform over the whole length. It is thinner between two nodes than at the nodes themselves, bulges out and has a slightly twisted shape. The non-uniform shape of the filaments could result in particle deposition [13,187]. It is proposed [13] that the main region of deposition would be around the point where the attached filaments bulge outward.

4.3. Filament torsion

As mentioned in the previous section, spacers in SWM modules of RO usually have torsion in filaments between two nodes of a mesh, which can result in the formation of longitudinal and transverse vortices, a more powerful destabilization of the concentration polarization layer and consequently a higher mass transfer. The torsion region of filaments is more obvious in thinner spacers than thicker ones (Fig. 6).

In heat transfer studies, modifying spacers by winding helical bars around cylindrical filaments or by using twisted tapes thought to enhance the mixing efficiencies of vortices close to the membrane walls [143]. However, these types of vortices occur mainly in the bulk of the flow, while the resistance against the mass transfer is greatest at the membrane walls [143]. Based on this, Li et al. [143] and Balster et al. [99] examined the torsion efficiency of spacers.

Surprisingly, Li et al. [143] found that spacers with modified filaments caused lower mass transfer than nonwoven net spacers. Balster et al. [99] found that spacers with twisted filaments have a higher mass transfer than unmodified spacers. However, in the study by Balster et al. [99], the geometric configuration of the spacers was not identical. Therefore, it seems that further investigation is required to elucidate the actual effect of torsion on not only the mass transfer but also on the pressure drop and fouling.

4.4. Location of transverse filaments

The position of transverse filaments in ladder and cavity spacers with respect to the channel height appears to be important for the mass transfer, energy usage, and fouling formation.

Geraldes et al. [172] investigated the formation of a concentration polarization layer on the membrane with respect to the position of transverse filaments in the channel height. Two scenarios were investigated: (i) in the first system, the transverse filaments were adjacent to the membrane and (ii) in the second system, the transverse filaments were placed on the impermeable layer on the opposite side of the membrane. The study assumed that the permeate flux along the membrane was uniform because both the osmotic pressure of the feed solution and the apparent rejection coefficient were low. A lower degree of concentration polarization was observed in the first scenario, where the same concentration polarization pattern was observed for each transverse filament, showing two maxima that appear in the base of each transverse filament. The first maximum, which was much higher, appears at the base of the filament positioned at the upstream of the inter-filament distance [172]. A PIV study showed that these are the locations with the lowest cross-section velocity [125].

However, the authors were unable to identify any experiment studies showing the effect positioning the transverse filaments at the middle of the channel with some distance from the top and bottom membrane (submerged spacers) on parameters such as concentration polarization, pressure drop and fouling. Cao et al. [164] discussed the effect of a ladder type submerged spacer through modeling. Using spacers with a transverse filament diameter 1/3 of the channel height ($d_{CT}/H_{CH} = 1/3$) at a Reynolds number between 120 and 480, the study [164] found that in contrast to zigzag spacers and ladder spacers, the flow in submerged spacers is symmetrical towards both membrane sheets, i.e. the mass transfer on both membrane sheets could have a similar magnitude.

4.5. Hydrodynamic angle (β)

The hydrodynamic angle is defined as the inner angle between two adjacent filaments facing the feed flow. The hydrodynamic angle ensures the generation of swirling in the feed channel albeit at the expense of an increase in the pressure drop [124,188]. The maximum cost [129] and a maximum flux are achieved by applying a spacer with a hydrodynamic angle of 90° [124] because a spacer with the hydrodynamic angle of 90° generates dominantly transverse vortices with an axis perpendicular to the flow direction [188]. Spacers with a hydrodynamic angle of 45° cause a degree of channeling either along the membrane surface or along the channel roof, which causes a flux reduction of 16–25% [129].

4.6. Spacer orientation

The spacer orientation is defined as the manner in which the flow attack angle faces the feed flow. Da Costa et al. [129] studied the effect of spacer orientation on the pressure drop and found that spacers with filaments parallel to the axis of the flow channel have a lower pressure drop and are therefore more economically attractive. Fimbbres-Weihs and Wiley [189] conducted a numerical study to show that the 45° orientation promotes mass transfer to a greater extent than that of the 90° orientation due to the absence of a fully formed recirculation region and an increase of wall shear by increase of the Reynolds number. Neal et al. [13] showed in an experimental study that flux in microfiltration membranes increases by increasing the flow attack angle, concluding that spacers with a flow attack angle of 45° have the best performance. This is attributed to two factors: (i) the tested spacer was made of two layers of nonwoven filaments with an hydrodynamic angle of 90° and (ii) positioning of the spacer for the highest possible angle (90°) on one membrane wall means the lowest possible angle of attack (0°) on the opposite membrane wall.

Neal et al. [13] studied the effects of spacer orientation on fouling for three scenarios: (i) when the transverse filaments were attached to the membrane and perpendicular to the flow (the 90° orientation), (ii) when the transverse filaments were attached to the membrane and parallel to the flow (0° orientation) and (iii) when the attached filaments were arranged at 45° of flow deposition (normal orientation). At 90° orientation, particles were deposited in a transverse band across the entire spacer cell, and the deposition region was displaced from the transverse filament by a zone of no deposition. The clear space between the edge of the filament and the deposition zone was attributed to the presence of recirculation eddies behind the transverse filaments. In the 0° orientation, orientation, particles were deposited by applying a higher flux, and deposition was concentrated around the attached filaments, which were parallel to the flow. In the normal orientation, deposition occurred mainly in the center of the cell. The location of the deposition was related to the shape of the filaments which were not uniform cylinders but instead wider at the center and edges.

4.7. Spacer thickness (channel height)

The height of a spacer-filled channel is determined by the thickness of the feed spacer. The channel height filled with nonwoven spacers is equal to the spacer's height at nodes where the transverse and longitudinal filaments cross each other. Theoretically, the spacer's height at each node is summation of a transverse and a longitudinal filament. Such estimation for channel height is used in most computational studies related to the nonwoven spacers. In practice, however, the spacer height at nodes is slightly smaller than the summation of transverse and longitudinal filaments because filaments at nodes are embedded within each other.

The increase of spacer thickness at a constant filament length results in a reduction of the porosity, specific surface area of the feed spacer and average velocity but an increase of the hydraulic diameter of the spacer. However, it is difficult to determine the effects of feed spacer thickness increase on the pressure drop by using theoretical formulas only.

The channel height determines the fouling formation at the membrane surface. At a constant flow rate, the cross-flow velocity in channels with thicker spacers is lower than channels with thinner spacers. A lower velocity means a thicker concentration polarization layer, a higher chance of particle deposition and a higher chance of scaling but a decreased chance of biofouling. The lower cross-flow velocity results in a lower nutrient load and consequently a lower biomass accumulation, a lower initial feed channel pressure drop and a lower increase of the feed channel pressure drop. The results of laboratory work [134], a pilot plan study [190] and a full-scale study [28] reveal that initial pressure drop decreases with the increase of feed spacer thickness. However, it should be noted that at a constant feed flow rate, the amount of biomass accumulation in channels with thinner spacers is the same as channels with thicker spacers because the amount of nutrient is constant [28,134,190]. In addition to the cross-flow velocity, the fouling will also be affected by the flow distribution pattern, which is a function of spacers' geometry, configuration and orientation.

Additionally, the membrane specific area is primarily determined by the feed spacer thickness. Membranes with larger specific area produce a larger quantity of water. Therefore, the spacer should be as thin as possible to have the largest possible membrane specific area and production rate but as thick as possible to cause the lowest possible pressure drop and fouling rate.

4.8. Number of filament layers

Standard nonwoven spacers are made of two layers of filaments on top of each other. One study argued that spacers with three filament layers are capable of increasing the flux without covering additional

membrane area, which led to lower capital and processing costs [98]. A comparison of 2-layer and 3-layer spacers of identical mesh length and hydraulic diameter showed that the 3-layer spacer operated at a higher flow instability range than the 2-layer spacer (lower Reynolds number power, n in Eq. (5)) but at the expense of higher pressure losses [98]. Li et al. [143] used multi-layer net-type spacers to investigate the effects of these type of spacers on the formation of the concentration polarization layer, process performance and cross-flow power consumption. They [143] concluded that the performance of multi-layer spacers was better than that of standard nonwoven spacers. One particular design of multi-layer spacers with standard nonwoven spacers in the outer layers and twisted tapes in the middle-layer showed an increase of 30% in Sherwood number compared to standard nonwoven spacers for the same cross-flow power consumption [143]. The same design showed 40% less power consumption at a constant Sherwood number compared to the standard nonwoven spacer.

The multilayer spacer designed by Balster et al. [99] was made of a standard net-type spacer in the middle and two thin net-type spacers on the outside. This design obtained 20% higher mass transfer compared to a standard nonwoven spacer at the same power consumption.

These selected studies did not investigate the effect of the multilayer spacer on the particulate fouling and biofouling.

4.9. Inter-filament distance and filament thickness

Da Costa et al. [15] reported that the mass transfer in the presence of spacers is a function of two mechanisms: (i) the friction generated by the mixing of fluid streams crossing each other at an angle, which is determined by the hydrodynamic angle of spacers and (ii) the friction created by wakes of fluid formed past transverse filaments. Under similar conditions, the second mechanism appears to be dominant and depends mainly on the filament shape and thickness [15], specifically demonstrating that thicker filaments had a higher impact on the mass transfer of the surface to which they are attached and are more likely to promote mass transfer on the opposite wall compared to thinner filaments. In a CFD study, Karode and Kumar [191] showed that spacers with unequal filament diameters caused a lower pressure drop and induced an unequal shear rate on the top and bottom faces of the flow channel. Such unequal shear rates at the top and bottom faces would be expected to have an adverse impact on the membrane module performance because of different mass transfer characteristics and fouling for adjacent membrane leaves. The study also found that a higher overall bulk instabilities flow would not necessarily result in higher shear rates at the top and bottom faces.

Shrivastava et al. [3] used ladder type spacers with a square cross-section in electrochemical flow cells to measure the current. The study reported that by decreasing the inter-filament spaces, the current transfer increased at the detached membrane and decreased at the attached membrane. The increase at the detached membrane is due to an increase in the number of filaments, an increase of the velocity above these filaments and an enhanced mass transfer. The decrease at the attached membrane is caused by reduction of the effective membrane area, which was occupied by the filaments.

It is common in the literature to use dimensionless values instead of filament diameter and inter-filament length. Relative height (d_{CP}/H_{CH}) and aspect ratio (l_{CP}/H_{CH}) are dimensionless terms that describe the ratio of filament height and inter-filament distance of transverse filaments to the channel height, respectively.

4.9.1. Relative height (d_{CP}/H_{CH})

The flow instabilities are, among other parameters, also a function of relative height and aspect ratio. Most nonwoven spacers are made with a relative height of 0.5. Geraldes et al. [149] showed that flow instabilities occur at $150 < Re < 300$ in a rectangular channel filled with a ladder-spacer that had a relative height of 0.5. Another finding of the study was that for a constant Reynolds number and aspect ratio (l_{CT}/H_{CH}), the decrease of relative height from 0.5 to 0.25 resulted in lower friction losses while the increase of relative height from 0.5 to 0.75 resulted in generation of a secondary recirculation region of significant dimension. This secondary recirculation region constituted a third type of flow structure, which was not observed for relative heights of 0.25 and 0.5. The third type of flow structure mentioned by Geraldes et al. [149] is likely a reason for mass transfer increase at thicker filaments mentioned by Da Costa et al. [15].

4.9.2. Aspect ratio

Cao et al. [164] suggested that reducing the transverse filament distance will reduce the distance between shear stress peaks. This was beneficial for the membrane mass transfer because the reduced distance between shear stress peaks introduced a larger shear stress near the membrane wall and increased the number of eddies.

Geraldes et al. [149] used ladder spacers with three aspect ratios, specifically 1.9, 3.8 and 5.7, to investigate the effect of mass transfer and friction losses. The friction number is decreased by decreasing the number of transverse filaments per unit length because of the decline of total drag of the fluid flow. In fact, all three contributors to the pressure drop in the cell (friction at the wall, friction at the surface of the filaments and friction due to the drag of the filaments) decrease with a reduction in the number of transverse filaments.

A higher flow instability close to the membrane wall indicates a higher mass transfer. Karode and Kumar [191] and Geraldes et al. [149] showed that an increase in aspect ratio (l_{CT}/H_{CH}) caused higher flow instabilities. Geraldes et al. [149] found that flow instabilities occur at lower Reynolds numbers for spacers with a constant relative height and greater aspect ratio. For instance, it was shown that the Reynolds numbers at which the instabilities start were $250 < Re < 300$, $175 < Re < 200$ and $150 < Re < 175$ for aspect ratios of 1.9, 3.8 and 5.7, respectively. In and Ho [171] reported that flow instabilities begin at a Reynolds number of 250–300 for zigzag type spacers and the cavity spacer with an aspect ratio of 5.

A high aspect ratio (l_{CT}/H_{CH}) led to the condition that the region of the recirculation zone, which occurs downstream of transverse filaments, did not reach the subsequent filament. Geraldes et al. [149] reported that for a constant relative height, the recirculation zone did not reach the subsequent transverse filament at aspect ratios 3.8 and 5.7.

Amokrane et al. [192] examined the effect of aspect ratio (d_{CT}/H_{CH}) for zigzag, cavity and submerged spacers with a constant relative height of 0.5 ($d_{CT}/H_{CH} = 0.5$). The study found that for aspect ratios (d_{CT}/H_{CH}) of 2 and 4, the flow remained stable in zigzag and cavity spacers but became unstable in submerged spacers. An additional finding was that the mass transfer through the membrane decreased in all three types of spacers by increasing the aspect ratio (d_{CT}/H_{CH}).

4.10. Spacer porosity

In SWM modules of RO where the top and bottom filaments are the same, the porosity is determined by knowing the aspect ratio (l_{CT}/H_{CH}) and hydrodynamic angle. Numerical methods showed a decreased pressure drop due to an increased aspect ratio and increased hydrodynamic angle [142]. Eq. (8) indicates that both an increase in the rate of l_{CT}/H_{CH} and a decrease in the hydrodynamic angle can translate into increased porosity. Therefore, an increase in the porosity results in a decrease of the pressure drop on one hand and an increase of flux due to greater active membrane area on the other. Da Costa et al. [129] reported that an increase of 70% in the porosity of a spacer led to a minor flux drop of 2–10% and minor pressure drop enhancement (see Table 8).

5. Conclusions

This work reviewed the effect of geometric design on the

Table 8
Summary of geometric effects of the feed spacer on the hydraulic conditions of the spacer-filled channel.

Investigated parameter	Specification	Results		
		Pressure drop	Flux	Fouling
Material	Adding metals	No remarkable changes	No noticeable change	Lower biofouling only in initial stages
	Polymer brushes	No remarkable changes	No noticeable changes	
Filament cross-section	Round filaments compare to other shapes	Lower pressure drop	Lower flux	–
Filament torsion		–	Flux enhancement due to destabilization of the boundary layer	–
Hydrodynamic angle in UF ($230 < Re < 1661$)	UF-90°	Highest pressure drop	Highest flux	–
	UF-45°		16–25% lower flux due to channeling	–
Orientation of feed spacer	45° versus 90°	45° had a higher pressure drop	45° had a better mass transfer	At 90° orientation, particles are deposited in a transverse band across the entire spacer cell, and in the normal orientation, deposition occurred primarily in the center of the cell
Spacer thickness	Increase from 0.7 to 0.86 mm	Lower pressure drop in thicker spacer	–	Lower fouling in thicker spacer
Number of layers		Higher turbulence and pressure drop	Higher flux	–
Relative height				
Aspect ratio	Increase of aspect ratio	Lower pressure drop		
Porosity	Increase of porosity	Minor decrease in pressure drop	Minor decrease in flux (2–10%)	

performance of SWM modules, generally, and the effect of feed spacer design on the hydraulic conditions of narrow feed channels and performance of SWM modules of RO in particular. Several researchers demonstrated the noteworthy effect of velocity on the fouling, the permeate production and pressure losses. The velocity in a spacer-filled channel is mostly affected by the feed spacer geometry. Therefore, it is crucial to understand how each parameter in spacer geometry affects the hydraulic conditions of the feed channel in order to be able to enhance the performance of the feed spacer and consequently the SWM modules.

This review shows that using of current feed spacers in SWM modules is beneficial for enhancing mass transfer and prevention of concentration polarization and scaling but it causes a more rapid particulate fouling and biofouling. Therefore, using a single type of spacer in SWM modules of RO for different applications is not beneficial and instead, it would be more advantageous to use a specific feed spacer for a particular type of feed water. For instance, the net-type spacer employed in the current SWM modules of RO is suitable for water with high salinity rather than water with low salinity at a determined recovery. This is because the net-type spacer can destabilize the concentration polarization layer to a reasonable extent by means of proper flow mixing, which also results in high pressure losses. However, the ratio of pressure losses to required feed pressure is almost negligible when applied to water with high salinity (high osmotic pressure). In contrast, the ratio of pressure losses to feed pressure becomes significantly higher in water with low salinity (low osmotic pressure), for which the concentration polarization is not the main problem. In contrast, the ladder-type spacers are more suitable for use with low salinity water such as river water because they have lower mixing ability and lower pressure losses compared to net-type spacers. The lower resistance of the ladder-type spacers also makes them more suitable to be cleaned with air-flow, by which the higher shear forces remove the particles and biofilms.

The detailed design of an optimal spacer for a specific type of feed water is possible by numerical studies and valued experimental studies with resolution in the range of numerical studies to validate them. There is a limited number of experimental techniques that can be used for validation of numerical studies in SWM modules of RO because the experimental studies often have a much lower resolution than numerical studies. Particle image velocimetry (PIV) is one of the techniques that can be used for validation of numerical studies.

References

[1] T. Oki, S. Kanae, Global hydrological cycles and world water resources, Science (2006) 1068–1072.
[2] I.A. Shiklomanov, World water resources, Water in Crisis, Oxford, New York, 1993.
[3] A. Shrivastava, S. Kumar, E.L. Cussler, Predicting the effect of membrane spacers on mass transfer, J. Membr. Sci. 323 (2008) 247–256.
[4] G. Grakist, C. Maas, W. Rosbergen, J.W.N.M. Kappelhof, Keeping our wells fresh, Proceedings of SWIM – 17, Delft University of Technology, Delft, 2002, pp. 337–340.
[5] K. Jena, Water Stress, Obituary, 2013, p. 12.
[6] L.F. Greenlee, D.F. Lawler, B.D. Freeman, B. Marrot, P. Moulin, Reverse osmosis desalination: water sources, technology, and today's challenges, Water Res. 43 (2009) 2317–2348.
[7] M. Uchymiak, A.R. Bartman, N. Daltrophe, M. Weissman, J. Gilron, P.D. Christofides, W.J. Kaiser, Y. Cohen, Brackish water reverse osmosis BWRO) operation in feed flow reversal mode using an ex situ scale observation detector (EXSOD), J. Membr. Sci. 341 (2009) 60–66.
[8] S. Belfer, Y. Purinson, R. Fainshtein, Y. Radchenko, O. Kedem, Surface modification of commercial composite polyamide reverse osmosis membranes, J. Membr. Sci. 139 (1998) 175–181.
[9] S. Belfer, Y. Purinson, O. Kedem, Surface modification of commercial polyamide reverse osmosis membranes by radical grafting: an ATR-FTIR study, Acta Polym. 49 (1998) 574–582.
[10] W. Byrne, Reverse Osmosis: A Practical Guide for Industrial Users, Tall Oaks Pub, 1995.
[11] DesalData, Forecast – DesalData, in, 2015.
[12] M.A. Eltawil, Z. Zhengming, L. Yuan, A review of renewable energy technologies integrated with desalination systems, Renew. Sustain. Energy Rev. 13 (2009)

2245–2262.
[13] P.R. Neal, H. Li, A.G. Fane, D.E. Wiley, The effect of filament orientation on critical flux and particle deposition in spacer-filled channels, J. Membr. Sci. 214 (2003) 165–178.
[14] J. Schwinge, P.R. Neal, D.E. Wiley, D.F. Fletcher, A.G. Fane, Spiral wound modules and spacers: review and analysis, J. Membr. Sci. (2004) 129–153.
[15] A.R. Da Costa, A.G. Fane, Net-type spacers: effect of configuration on fluid flow path and ultrafiltration flux, Indust. Eng. Chem. Res. (1994) 1845–1851.
[16] C.P. Koutsou, S.G. Yiantsios, A.J. Karabelas, Numerical simulation of the flow in a plane-channel containing a periodic array of cylindrical turbulence promoters, J. Membr. Sci. 231 (2004) 81–90.
[17] J. Kucera, Membranes, Reverse Osmosis, John Wiley & Sons, Inc., 2015, pp. 49–93.
[18] L.A. Lien, Spiral-wound membrane with improved permeate carrier, in, Google Patents, 1989.
[19] G. Schock, A. Miquel, Mass transfer and pressure loss in spiral wound modules, Desalination 64 (1987) 339–352.
[20] C.P. Koutsou, A.J. Karabelas, M. Kostoglou, Membrane desalination under constant water recovery – the effect of module design parameters on system performance, Sep. Purif. Technol. 147 (2015) 90–113.
[21] W.G.J. Van der Meer, Mathematical Modelling of NF and RO Membrane Filtration Plants and Modules, 2003.
[22] J.C. Crittenden, R.R. Trussell, D.W. Hand, K.J. Howe, G. Tchobanoglous, Membrane Filtration, MWH's Water Treatment: Principles and Design, third ed., John Wiley & Sons, Inc., 2012, pp. 819–902.
[23] C.C. Zimmerer, V. Kottke, Effects of spacer geometry on pressure drop, mass transfer, mixing behavior, and residence time distribution, Desalination 104 (1996) 129–134.
[24] J. Johnson, M. Busch, Engineering aspects of reverse osmosis module design, Desal. Water Treat. 15 (2010) 236–248.
[25] W.G.J. van der Meer, J.A.M. van Paassen, M.C. Riemersma, F.o.H.J. van Ekkendonk, Optiflux®: from innovation to realisation, Desalination (2003) 159–165.
[26] J.A.M. van Paassen, W.G.J. van der Meer, J. Post, Optiflux®: from innovation to realisation, Desalination (2005) 325–331.
[27] J.S. Vrouwenvelder, M.C.M. van Loosdrecht, J.C. Kruithof, A novel scenario for biofouling control of spiral wound membrane systems, Water Res. 45 (2011) 3890–3898.
[28] C. Bartels, M. Hirose, H. Fujioka, Performance advancement in the spiral wound RO/NF element design, in: Desalination European Desalination Society and Center for Research and Technology Hellas (CERTH), Sani Resort 22-25 April 2007, Halkidiki, Greece European Desalination Society and Center for Research and Technology Hellas (CERTH), Sani Resort, 2008, pp. 207–214.
[29] H.Y. Ng, S.L. Ong, A novel 400-mm RO system for water reuse and desalination, J. Environ. Eng. Manage. 17 (2007) 113.
[30] C. Fritzmann, J. Löwenberg, T. Wintgens, T. Melin, State-of-the-art of reverse osmosis desalination, Desalination 216 (2007) 1–76.
[31] R. Franks, C. Bartels, A. Anit, Demonstrating improved RO system performance with new Low Differential (LD) technology, in: Hydranautics, Hydranautics, Oceanside, CA., 2010.
[32] M. Busch, W.E. Mickols, Reducing energy consumption in seawater desalination, Desalination 165 (2004) 299–312.
[33] V.G. Molina, M. Busch, P. Sehn, Cost savings by novel seawater reverse osmosis elements and design concepts, Desalination Water Treat. 7 (2009) 160–177.
[34] K.P. Lee, T.C. Arnot, D. Mattia, A review of reverse osmosis membrane materials for desalination—development to date and future potential, J. Membr. Sci. 370 (2011) 1–22.
[35] J.T. Arena, B. McCloskey, B.D. Freeman, J.R. McCutcheon, Surface modification of thin film composite membrane support layers with polydopamine: enabling use of reverse osmosis membranes in pressure retarded osmosis, J. Membr. Sci. 375 (2011) 55–62.
[36] J. Gilron, S. Belfer, P. Väisänen, M. Nyström, Effects of surface modification on antifouling and performance properties of reverse osmosis membranes, Desalination 140 (2001) 167–179.
[37] G. Kang, M. Liu, B. Lin, Y. Cao, Q. Yuan, A novel method of surface modification on thin-film composite reverse osmosis membrane by grafting poly(ethylene glycol), Polymer 48 (2007) 1165–1170.
[38] Q. Li, Z. Xu, I. Pinnau, Fouling of reverse osmosis membranes by biopolymers in wastewater secondary effluent: Role of membrane surface properties and initial permeate flux, J. Membr. Sci. 290 (2007) 173–181.
[39] J.S. Louie, I. Pinnau, I. Ciobanu, K.P. Ishida, A. Ng, M. Reinhard, Effects of polyether–polyamide block copolymer coating on performance and fouling of reverse osmosis membranes, J. Membr. Sci. 280 (2006) 762–770.
[40] X. Wei, Z. Wang, J. Chen, J. Wang, S. Wang, A novel method of surface modification on thin-film-composite reverse osmosis membrane by grafting hydantoin derivative, J. Membr. Sci. 346 (2010) 152–162.
[41] M. Mulder, Basic Principles of Membrane Technology, Kluwer Academic, 1991.
[42] S. Sourirajan, WATER FRXM SALINE, in, Google Patents, 1964.
[43] J.E. Cadotte, Interfacially synthesized reverse osmosis membrane, in, Google Patents, 1981.
[44] J.E. Cadotte, R.S. King, R.J. Majerle, R.J. Petersen, Interfacial synthesis in the preparation of reverse osmosis membranes, J. Macromol. Sci.: Part A – Chem. (1981) 727–755.
[45] W. Kamin'ski, J. Stawczyk, An effect of vortex flow on fluxes in ultrafiltration plate-frame modules, J. Membr. Sci. 123 (1997) 157–164.
[46] M.F.A. Goosen, S.S. Sablani, H. Al-Hinai, S. Al-Obeidani, R. Al-Belushi, D. Jackson, Fouling of reverse osmosis and ultrafiltration membranes: a critical review, Sep. Sci. Technol. (2005) 2261–2297.
[47] J.S. Vrouwenvelder, J.A.M. van Paassen, L.P. Wessels, A.F. van Dam, S.M. Bakker, The membrane fouling simulator: a practical tool for fouling prediction and control, J. Membr. Sci. 281 (2006) 316–324.
[48] J. Vrouwenvelder, C. Hinrichs, A. Sun, F. Royer, J. van Paassen, S. Bakker, W. van der Meer, J. Kruithof, M. van Loosdrecht, Monitoring and control of biofouling in nanofiltration and reverse osmosis membranes, 2008
[49] J.A. Howell, The Membrane Alternative: Energy Implications for Industry: Watt Committee Report Number 21, Taylor & Francis, 1990.
[50] S. Shirazi, C.-J. Lin, D. Chen, Inorganic fouling of pressure-driven membrane processes — a critical review, Desalination 250 (2010) 236–248.
[51] L. Song, K. Tay, Advanced Membrane Fouling Characterization in Full-Scale Reverse Osmosis Processes, in: L.K. Wang, J.P. Chen, Y.T. Hung, N.K. Shammas (Eds.), Membrane and Desalination Technologies, Humana Press, 2008, pp. 101–134.
[52] H.F. Ridgway, A. Kelly, C. Justice, B.H. Olson, Microbial fouling of reverse-osmosis membranes used in advanced wastewater treatment technology: chemical, bacteriological, and ultrastructural analyses, Appl. Environ. Microbiol. 45 (1983) 1066–1084.
[53] R.P. Schneider, L.M. Ferreira, P. Binder, E.M. Bejarano, K.P. Góes, E. Slongo, C.R. Machado, G.M.Z. Rosa, Dynamics of organic carbon and of bacterial populations in a conventional pretreatment train of a reverse osmosis unit experiencing severe biofouling, J. Membr. Sci. 266 (2005) 18–29.
[54] J.S. Baker, L.Y. Dudley, Biofouling in membrane systems – a review, in: Desalination, Conference Membranes in Drinking and Industrial Water Production, 1998, pp. 81–89.
[55] K. Tasaka, T. Katsura, H. Iwahori, Y. Kamiyama, Analysis of RO elements operated at more than 80 plants in Japan, in: Desalination, Proceedings of the IDA and WRPC World Conference on Desalination and Water Treatment, 1994, pp. 259–272.
[56] C.L. Chen, W.T. Liu, M.L. Chong, M.T. Wong, S.L. Ong, H. Seah, W.J. Ng, Community structure of microbial biofilms associated with membrane-based water purification processes as revealed using a polyphasic approach, Appl. Microbiol. Biotechnol. (2004) 466–473.
[57] L.A. Bereschenko, G.H.J. Heilig, M.M. Nederlof, M.C.M. van Loosdrecht, A.J.M. Stams, G.J.W. Euverink, Molecular characterization of the bacterial communities in the different compartments of a full-scale reverse-osmosis water purification plant, Appl. Environ. Microbiol. 74 (2008) 5297–5304.
[58] H.C. Flemming, G. Schaule, T. Griebe, J. Schmitt, A. Tamachkiarowa, Biofouling-the Achilles heel of membrane processes, in: Desalination, Workshop on Membranes in Drinking Water Production Technical Innovations and Health Aspects, 1997, pp. 215–225.
[59] S. Tsuneda, H. Aikawa, H. Hayashi, A. Yuasa, A. Hirata, Extracellular polymeric substances responsible for bacterial adhesion onto solid surface, FEMS Microbiol. Lett. 223 (2003) 287–292.
[60] J.W. Costerton, P.S. Stewart, E.P. Greenberg, Bacterial biofilms: a common cause of persistent infections, Science 284 (1999) 1318–1322.
[61] J.S. Vrouwenvelder, D. Van Der Kooij, Integral diagnosis of fouling problems by analysing biomass and inorganic compounds in membrane elements used in water treatment, Water Sci. Technol.: Water Supply (2003) 211–215.
[62] M.C. Van Loosdrecht, J. Lyklema, W. Norde, A.J. Zehnder, Influence of interfaces on microbial activity, Microbiol. Rev. 54 (1990) 75–87.
[63] A. Gjaltema, N. van der Marel, M.C.M. van Loosdrecht, J.J. Heijnen, Adhesion and biofilm development on suspended carriers in airlift reactors: hydrodynamic conditions versus surface characteristics, Biotechnol. Bioeng. 55 (1997) 880–889.
[64] O. Holm-Hansen, C.R. Booth, The measurement of adenosine triphosphate in the ocean and its ecological significance, Limnol. Oceanogr. (1966) 510–519.
[65] S. Kim, S. Lee, S. Hong, Y. Oh, M. Seoul, J. Kweon, T. Kim, Biofouling of reverse osmosis membranes: microbial quorum sensing and fouling propensity, Desalination 247 (2009) 303–315.
[66] C. Coufort, N. Derlon, J. Ochoa-Chaves, A. Line, E. Paul, Cohesion and detachment in biofilm systems for different electron acceptor and donors, Water Sci. Technol. 55 (2007) 421–428.
[67] J. Mansouri, S. Harrisson, V. Chen, Strategies for controlling biofouling in membrane filtration systems: challenges and opportunities, J. Mater. Chem. 20 (2010) 4567–4586.
[68] J.S. Vrouwenvelder, S.A. Manolarakis, J.P. van der Hoek, J.A.M. van Paassen, W.G.J. van der Meer, J.M.C. van Agtmaal, H.D.M. Prummel, J.C. Kruithof, M.C.M. van Loosdrecht, Quantitative biofouling diagnosis in full scale nanofiltration and reverse osmosis installations, Water Res. 42 (2008) 4856–4868.
[69] D.A. Graf von der Schulenburg, J.S. Vrouwenvelder, S.A. Creber, M.C.M. van Loosdrecht, M.L. Johns, Nuclear magnetic resonance microscopy studies of membrane biofouling, J. Membr. Sci. 323 (2008) 37–44.
[70] E.R. Cornelissen, J.S. Vrouwenvelder, S.G.J. Heijman, X.D. Viallefont, D. Van Der Kooij, L.P. Wessels, Periodic air/water cleaning for control of biofouling in spiral wound membrane elements, J. Membr. Sci. 287 (2007) 94–101.
[71] J.S. Vrouwenvelder, J.A.M. van Paassen, J.M.C. van Agtmaal, M.C.M. van Loosdrecht, J.C. Kruithof, A critical flux to avoid biofouling of spiral wound nanofiltration and reverse osmosis membranes: fact or fiction? J. Membr. Sci. 326 (2009) 36–44.
[72] P. Moulin, J.C. Rouch, C. Serra, M.J. Clifton, P. Aptel, Mass transfer improvement by secondary flows: dean vortices in coiled tubular membranes, J. Membr. Sci. 114 (1996) 235–244.
[73] H.B. Winzeler, G. Belfort, Enhanced performance for pressure-driven membrane processes: the argument for fluid instabilities, J. Membr. Sci. 80 (1993) 35–47.
[74] G. Belfort, R.H. Davis, A.L. Zydney, The behavior of suspensions and

macromolecular solutions in crossflow microfiltration, J. Membr. Sci. 96 (1994) 1–58.
[75] S. Wäsche, N.H. Horn, D.C. Hempel, Influence of growth conditions on biofilm development and mass transfer at the bulk/biofilm interface, Water Res. 36 (2002) 4775–4784.
[76] S. Wijeyekoon, T. Mino, H. Satoh, T. Matsuo, Effects of substrate loading rate on biofilm structure, Water Res. 38 (2004) 2479–2488.
[77] M.C.M. van Loosdrecht, D. Eikelboom, A. Gjaltema, A. Mulder, L. Tijhuis, J.J. Heijnen, Biofilm structures, in: Water Science and Technology, Biofilm Structure, Growth and Dynamics Selected Proceedings of the IAWQ International Conference and Workshop on Biofilm Structure, Growth and Dynamics, 1995, pp. 35–43.
[78] B.M. Peyton, Effects of shear stress and substrate loading rate on Pseudomonas aeruginosa biofilm thickness and density, Water Res. 30 (1996) 29–36.
[79] W.K. Kwok, C. Picioreanu, S.L. Ong, M.C.M. van Loosdrecht, W.J. Ng, J.J. Heijnen, Influence of biomass production and detachment forces on biofilm structures in a biofilm airlift suspension reactor, Biotechnol. Bioeng. 58 (1998) 400–407.
[80] L.F. Melo, T.R. Bott, Biofouling in water systems, in: Experimental Thermal and Fluid Science, Heat Exchange Fouling, 1997, pp. 375–381.
[81] M.O. Pereira, M. Kuehn, S. Wuertz, T. Neu, L.F. Melo, Effect of flow regime on the architecture of a Pseudomonas fluorescens biofilm, Biotechnol. Bioeng. 78 (2002) 164–171.
[82] J.J. Beun, A. Hendriks, M.C.M. van Loosdrecht, E. Morgenroth, P.A. Wilderer, J.J. Heijnen, Aerobic granulation in a sequencing batch reactor, Water Res. 33 (1999) 2283–2290.
[83] M.J. Chen, Z. Zhang, T.R. Bott, Effects of operating conditions on the adhesive strength of Pseudomonas fluorescens biofilms in tubes, Colloids Surf., B 43 (2005) 61–71.
[84] B. Purevdorj, J.W. Costerton, P. Stoodley, Influence of Hydrodynamics and Cell Signaling on the Structure and Behavior of Pseudomonas aeruginosa Biofilms, Appl. Environ. Microbiol. 68 (2002) 4457–4464.
[85] P.A. Araùjo, D.J. Miller, P.B. Correia, M.C.M. van Loosdrecht, J.C. Kruithof, B.D. Freeman, D.R. Paul, J.S. Vrouwenvelder, Impact of feed spacer and membrane modification by hydrophilic, bactericidal and biocidal coating on biofouling control, Desalination 295 (2012) 1–10.
[86] J.S. Vrouwenvelder, J. Buiter, M. Riviere, W.G.J. van der Meer, M.C.M. van Loosdrecht, J.C. Kruithof, Impact of flow regime on pressure drop increase and biomass accumulation and morphology in membrane systems, Water Res. 44 (2010) 689–702.
[87] J.Y. Park, C.K. Choi, J.J. Kim, A study on dynamic separation of silica slurry using a rotating membrane filter 1. Experiments and filtrate fluxes, J. Membr. Sci. 97 (1994) 263–273.
[88] L. Ding, C. Charcosset, M. Jaffrin, Albumin recovery enhancement in membrane plasma fractionation using pulsatile flow, Int. J. Artif. Organs 14 (1991) 61–65.
[89] Y. Wang, J.A. Howell, R.W. Field, D. Wu, Simulation of cross-flow filtration for baffled tubular channels and pulsatile flow, J. Membr. Sci. 95 (1994) 243–258.
[90] W.S. Kim, J.K. Park, H.N. Chang, Mass transfer in a three-dimensional net-type turbulence promoter, Int. J. Heat Mass Transfer 30 (1987) 1183–1192.
[91] J. Balster, D.F. Stamatialis, M. Wessling, Towards spacer free electrodialysis, J. Membr. Sci. 341 (2009) 131–138.
[92] K. Zhang, Z. Cui, R.W. Field, Effect of bubble size and frequency on mass transfer in flat sheet MBR, J. Membr. Sci. 332 (2009) 30–37.
[93] S. Judd, The MBR Book: Principles and Applications of Membrane Bioreactors for Water and Wastewater Treatment, Elsevier, 2010.
[94] N.V. Ndinisa, A.G. Fane, D.E. Wiley, Fouling control in a submerged flat sheet membrane system: Part I – bubbling and hydrodynamic effects, Sep. Sci. Technol. (2006) 1383–1409.
[95] N.V. Ndinisa, A.G. Fane, D.E. Wiley, D.F. Fletcher, Fouling control in a submerged flat sheet membrane system: Part II – two-phase flow characterization and CFD simulations, Sep. Sci. Technol. (2006) 1411–1445.
[96] N.V. Ndinisa, A.G. Fane, D.E. Wiley, Fouling control in a submerged flat sheet membrane system: Part I – bubbling and hydrodynamic effects, Sep. Sci. Technol. 41 (2006) 1383–1409.
[97] C. Fritzmann, M. Hausmann, M. Wiese, M. Wessling, T. Melin, Microstructured spacers for submerged membrane filtration systems, J. Membr. Sci. 446 (2013) 189–200.
[98] J. Schwinge, D.E. Wiley, A.G. Fane, Novel spacer design improves observed flux, J. Membr. Sci. 229 (2004) 53–61.
[99] J. Balster, I. Pünt, D.F. Stamatialis, M. Wessling, Multi-layer spacer geometries with improved mass transport, J. Membr. Sci. 282 (2006) 351–361.
[100] D. Kim, S. Jung, J. Sohn, H. Kim, S. Lee, Biocide application for controlling biofouling of SWRO membranes – an overview, in: Desalination, Issues 1 and 2: First International Workshop between the Center for the Seawater Desalination Plant and the European Desalination Society First International Workshop between the Center for the Seawater Desalination Plant and the European Desalination Society, 2009, pp. 43–52.
[101] C. Whittaker, H. Ridgway, B.H. Olson, Evaluation of cleaning strategies for removal of biofilms from reverse-osmosis membranes, Appl. Environ. Microbiol. 48 (1984) 395–403.
[102] A. Al-Amoudi, R.W. Lovitt, Fouling strategies and the cleaning system of NF membranes and factors affecting cleaning efficiency, J. Membr. Sci. 303 (2007) 4–28.
[103] E. Zondervan, B. Roffel, Evaluation of different cleaning agents used for cleaning ultra filtration membranes fouled by surface water, J. Membr. Sci. 304 (2007) 40–49.
[104] S. Patil, F. Harnisch, U. Schröder, Toxicity response of electroactive microbial biofilms-a decisive feature for potential biosensor and power source applications, ChemPhysChem 11 (2010) 2834–2837.
[105] R. Hausman, T. Gullinkala, I.C. Escobar, Development of copper-charged polypropylene feedspacers for biofouling control, J. Membr. Sci. 358 (2010) 114–121.
[106] H. Winters, L. Isquith, A critical evaluation of pretreatment to control fouling in open seawater reverse osmosis—has it been a success?, in: In Proceedings of the International Desalination Association World Congress on Desalination and Water Reuse, Abu Dhabi, UAE, 1995, pp. 255–264.
[107] L.E. Applegate, C.W. Erkenbrecher, H. Winters, New chloroamine process to control aftergrowth and biofouling in permasepR B-10 RO surface seawater plants, Desalination 74 (1989) 51–67.
[108] H. Winters, Twenty years experience in seawater reverse osmosis and how chemicals in pretreatment affect fouling of membranes, Desalination 110 (1997) 93–96.
[109] S. Selvaraj, K.C. Saha, A. Chakraborty, S.N. Bhattacharyya, A. Saha, Toxicity of free and various aminocarboxylic ligands sequestered copper(II) ions to *Escherichia coli*, J. Hazard. Mater. 166 (2009) 1403–1409.
[110] B.R. Kim, J.E. Anderson, S.A. Mueller, W.A. Gaines, A.M. Kendall, Literature review–efficacy of various disinfectants against Legionella in water systems, Water Res. 36 (2002) 4433–4444.
[111] K. Garny, T.R. Neu, H. Horn, Sloughing and limited substrate conditions trigger filamentous growth in heterotrophic biofilms–measurements in flow-through tube reactor, Chem. Eng. Sci. 64 (2009) 2723–2732.
[112] R.P. Carnahan, L. Bolin, W. Suratt, Biofouling of PVD-1 reverse osmosis elements in the water treatment plant of the City of Dunedin, Florida, in: Desalination: Proceedings of the American Desalting Association 1994 Biennial Conference and Exposition Membrane and Desalting Technologies, 1995, pp. 235–244.
[113] Z. Cui, T. Taha, Enhancement of ultrafiltration using gas sparging: a comparison of different membrane modules, J. Chem. Technol. Biotechnol. 78 (2003) 249–253.
[114] J.Q.J.C. Verberk, P. Hoogeveen, H. Futselaar, J. van Dijk, Hydraulic distribution of water and air over a membrane module using AirFlush, Water Supply 2 (2002) 297–304.
[115] L. Tijhuis, B. Hijman, M.C.M. Loosdrecht, J.J. Heijnen, Influence of detachment, substrate loading and reactor scale on the formation of biofilms in airlift reactors, Appl Microbiol Biotechnol (1996) 7–17.
[116] J.W. Kappelhof, H.S. Vrouwenvelder, M. Schaap, J.C. Kruithof, D. Van Der Kooij, J.C. Schippers, An in situ biofouling monitor for membrane systems, Water Sci. Technol.: Water Suppl. (2003) 205–210.
[117] P. Willems, N.G. Deen, A.J.B. Kemperman, R.G.H. Lammertink, M. Wessling, M. van Sint Annaland, J.A.M. Kuipers, W.G.J. van der Meer, Use of Particle Imaging Velocimetry to measure liquid velocity profiles in liquid and liquid/gas flows through spacer filled channels, J. Membr. Sci. 362 (2010) 143–153.
[118] I.S. Ngene, R.G.H. Lammertink, A.J.B. Kemperman, W.J.C. van de Ven, L.P. Wessels, M. Wessling, W.G.J. Van der Meer, CO_2 nucleation in membrane spacer channels remove biofilms and fouling deposits, Indust. Eng. Chem. Res. (2010) 10034–10039.
[119] T.S. Coffey, Diet Coke and Mentos: what is really behind this physical reaction? Am. J. Phys. 76 (2008) 551–557.
[120] M. Wilf, Effect of new generation of low pressure, high salt rejection membranes on power consumption of RO systems, in: American Water Works Association, Membrane Technology Conference, New Orleans, LA, 1997.
[121] A.J. Karabelas, Key issues for improving the design and operation of spiral-wound membrane modules in desalination plants, Desalination Water Treat. 52 (2014) 1820–1832.
[122] M. Wilf, C. Bartels, Optimization of seawater RO systems design, Desalination 173 (2005) 1–12.
[123] T.S.o. RO-Chemicals, Net Driving Pressure – Reverse Osmosis Systems, in, RO-Chemicals.
[124] A.R. Da Costa, A.G. Fane, D.E. Wiley, Spacer characterization and pressure drop modelling in spacer-filled channels for ultrafiltration, J. Membr. Sci. 87 (1994) 79–98.
[125] A.H. Haidari, S.G.J. Heijman, W.G.J. van der Meer, Visualization of hydraulic conditions inside the feed channel of Reverse Osmosis: a practical comparison of velocity between empty and spacer-filled channel, Water Res. 106 (2016) 232–241.
[126] G. Belfort, G.A. Guter, An experimental study of electrodialysis hydrodynamics, Desalination 10 (1972) 221–262.
[127] D.G. Thomas, P.H. Hayes, W.R. Mixon, J.D. Sheppard, W.L. Griffith, R.M. Keller, Turbulence promoters for hyperfiltration with dynamic membranes, Environ. Sci. Technol. (1970) 1129–1136.
[128] W.G. Light, T.V. Tran, Improvement of thin-channel design for pressure-driven membrane systems, Indust. Eng. Chem. Process Des. Dev. (1981) 33–40.
[129] A.R. Da Costa, A.G. Fane, C.J.D. Fell, A.C.M. Franken, Optimal channel spacer design for ultrafiltration, J. Membr. Sci. 62 (1991) 275–291.
[130] S.V. Polyakov, F.N. Karelin, Turbulence promoter geometry: its influence on salt rejection and pressure losses of a composite-membrane spiral would module, J. Membr. Sci. 75 (1992) 205–211.
[131] J. Schwinge, D.E. Wiley, A.G. Fane, R. Guenther, Characterization of a zigzag spacer for ultrafiltration, J. Membr. Sci. 172 (2000) 19–31.
[132] R.F. Probstein, J.S. Shen, W.F. Leung, Ultrafiltration of macromolecular solutions at high polarization in laminar channel flow, Desalination 24 (1977) 1–16.
[133] J.J.S. Shen, R.F. Probstein, Turbulence promotion and hydrodynamic optimization in an ultrafiltration process, Indust. Eng. Chem. Process Des. Dev. (1979) 547–554.
[134] P.A. Araújo, J.C. Kruithof, M.C.M. van Loosdrecht, J.S. Vrouwenvelder, The potential of standard and modified feed spacers for biofouling control, J. Membr. Sci. 403–404 (2012) 58–70.
[135] I.S. Ngene, R.G.H. Lammertink, M. Wessling, W.G.J. Van der Meer, Particle

deposition and biofilm formation on microstructured membranes, J. Membr. Sci. 364 (2010) 43–51.
[136] D.G. Thomas, Forced convection mass transfer in hyperfiltration at high fluxes, Indust. Eng. Chem. Fundam. (1973) 396–405.
[137] O. Kuroda, S. Takahashi, M. Nomura, Characteristics of flow and mass transfer rate in an electrodialyzer compartment including spacer, Desalination 46 (1983) 225–232.
[138] F. Schwager, P.M. Robertson, N. Ibl, The use of eddy promoters for the enhancement of mass transport in electrolytic cells, Electrochim. Acta 25 (1980) 1655–1665.
[139] H. Chang, J.-A. Hsu, C.-L. Chang, C.-D. Ho, CFD study of heat transfer enhanced membrane distillation using spacer-filled channels, Energy Proc. 75 (2015) 3213–3219.
[140] R. Darby, Chemical Engineering Fluid Mechanics, Taylor & Francis, Revised and Expanded, 2001.
[141] P. Feron, G.S. Solt, The influence of separators on hydrodynamics and mass transfer in narrow cells: flow visualisation, Desalination 84 (1991) 137–152.
[142] C.P. Koutsou, S.G. Yiantsios, A.J. Karabelas, Direct numerical simulation of flow in spacer-filled channels: effect of spacer geometrical characteristics, J. Membr. Sci. 291 (2007) 53–69.
[143] F. Li, W. Meindersma, A.B. de Haan, T. Reith, Novel spacers for mass transfer enhancement in membrane separations, J. Membr. Sci. 253 (2005) 1–12.
[144] M.S. Isaacson, A.A. Sonin, Sherwood number and friction factor correlations for electrodialysis systems, with application to process optimization, Indust. Eng. Chem. Process Des. Dev. (1976) 313–321.
[145] P. Hickey, Gooding, CH, Proceedings of Sixth International Conference on Pervaporation Processes in the Chemical Industry, in: B.M. Corporation (Ed.), Pervaporation processes in the chemical industry, Bakish Materials Corporation, Ottawa, Canada, 1992, pp. 153–169.
[146] D. Van Gauwbergen, J. Baeyens, Macroscopic fluid flow conditions in spiral-wound membrane elements, Desalination 110 (1997) 287–299.
[147] J. Du Plessis, M. Collins, A new definition for laminar flow entrance lengths of straight ducts, N & O J. 25 (1992) 11–16.
[148] C. Berner, F. Durst, D.M. McEligot, Flow around baffles, J. Heat Transfer 106 (1984) 743–749.
[149] V. Geraldes, V. Semião, M.N. de Pinho, Flow management in nanofiltration spiral wound modules with ladder-type spacers, J. Membr. Sci. 203 (2002) 87–102.
[150] R.B. Bird, W.E. Stewart, E.N. Lightfoot, Transport Phenomena, Wiley, 2007.
[151] E. Pellerin, E. Michelitsch, K. Darcovich, S. Lin, C.M. Tam, Turbulent transport in membrane modules by CFD simulation in two dimensions, J. Membr. Sci. 100 (1995) 139–153.
[152] G.A. Fimbres-Weihs, D.E. Wiley, Review of 3D CFD modeling of flow and mass transfer in narrow spacer-filled channels in membrane modules, in: Chemical Engineering and Processing: Process Intensification, Process Intensification on Intensified Transport by Complex Geometries, 2010, pp. 759–781.
[153] F.R. Menter, Two-equation eddy-viscosity turbulence models for engineering applications, AIAA J. 32 (1994) 1598–1605.
[154] V. Yakhot, S.A. Orszag, Renormalization group analysis of turbulence. I. Basic theory, J. Sci. Comput. 1 (1986) 3–51.
[155] A.A. Sonin, M.S. Isaacson, Optimization of flow design in forced flow electrochemical systems, with special application to electrodialysis, Indust. Eng. Chem. Process Des. Dev. (1974) 241–248.
[156] Y. Winograd, A. Solan, M. Toren, Mass transfer in narrow channels in the presence of turbulence promoters, Desalination 13 (1973) 171–186.
[157] D.G. Thomas, J.S. Watson, Hyperfiltration. Reduction of concentration polarization of dynamically formed hyperfiltration membranes by detached turbulence promoters, Indust. Eng. Chem. Process Des. Dev. (1968) 397–401.
[158] D.G. Thomas, W.R. Mixon, Effect of axial velocity and initial flux on flux decline of cellulose acetate membranes in hyperfiltration of primary sewage effluents, Indust. Eng. Chem. Process Des. Dev. (1972) 339–343.
[159] D.G. Thomas, Estimation of concentration polarization for ion-exclusion hyperfiltration membranes with turbulent flow, Indust. Eng. Chem. Fundam. (1972) 302–307.
[160] J.J.S. Shen, R.F. Probstein, On the prediction of limiting flux in laminar ultrafiltration of macromolecular solutions, Indust. Eng. Chem. Fundam. (1977) 459–465.
[161] Y. Taniguchi, An analysis of reverse osmosis characteristics of ROGA spiral-wound modules, Desalination 25 (1978) 71–88.
[162] J.L.C. Santos, V. Geraldes, S. Velizarov, J.G. Crespo, Investigation of flow patterns and mass transfer in membrane module channels filled with flow-aligned spacers using computational fluid dynamics CFD, J. Membr. Sci. 305 (2007) 103–117.
[163] H. Ohya, Y. Taniguchi, An analysis of reverse osmotic characteristics of ROGA-4000 spiral-wound module, Desalination 16 (1975) 359–373.
[164] Z. Cao, D.E. Wiley, A.G. Fane, CFD simulations of net-type turbulence promoters in a narrow channel, J. Membr. Sci. 185 (2001) 157–176.
[165] J.S. Vrouwenvelder, S.M. Bakker, L.P. Wessels, J.A.M. van Paassen, The Membrane Fouling Simulator as a new tool for biofouling control of spiral-wound membranes, in: Desalination, EuroMed 2006 Conference on Desalination Strategies in South Mediterranean Countries, 2007, pp. 170–174.
[166] S.A. Creber, J.S. Vrouwenvelder, M.C.M. van Loosdrecht, M.L. Johns, Chemical cleaning of biofouling in reverse osmosis membranes evaluated using magnetic resonance imaging, J. Membr. Sci. 362 (2010) 202–210.
[167] S. Avlonitis, W.T. Hanbury, M.B. Boudinar, Spiral wound modules performance. An analytical solution, part I, in: Desalination, Proceedings of the Twelfth International Symposium on Desalination and Water Re-use, 1991, pp. 191–208.
[168] S. Avlonitis, W.T. Hanbury, M.B. Boudinar, Spiral wound modules performance an analytical solution: Part II, Desalination 89 (1993) 227–246.
[169] G.A.F. Weihs, Numerical Simulation Studies of Mass Transfer under Steady and Unsteady Fluid Flow in Two- and Three-Dimensional Spacer-Filled Channels, School of Chemical Sciences and Engineering UNESCO Centre for Membrane Science and Technology, The University of New South Wales, Sydney, Australia, 2008, p. 212.
[170] R. Ghidossi, D. Veyret, P. Moulin, Computational fluid dynamics applied to membranes: state of the art and opportunities, Chem. Eng. Process. 45 (2006) 437–454.
[171] S.K. In, N.C. Ho, The effect of turbulence promoters on mass transfer – numerical analysis and flow visualization, Int. J. Heat Mass Transfer 25 (1982) 1167–1181.
[172] V. Geraldes, V. Semião, M.N. de Pinho, The effect of the ladder-type spacers configuration in NF spiral-wound modules on the concentration boundary layers disruption, Desalination 146 (2002) 187–194.
[173] C. Gaucher, P. Legentilhomme, P. Jaouen, J. Comiti, J. Pruvost, Hydrodynamics study in a plane ultrafiltration module using an electrochemical method and particle image velocimetry visualization, Exp. Fluids (2002) 283–293.
[174] M. Raffel, C.E. Willert, J. Kompenhans, Particle Image Velocimetry: A Practical Guide, Springer, 1998.
[175] R.J. Adrian, Twenty years of particle image velocimetry, Exp. Fluids (2005) 159–169.
[176] M. Gimmelshtein, R. Semiat, Investigation of flow next to membrane walls, J. Membr. Sci. 264 (2005) 137–150.
[177] M. Oinuma, S. Sawada, K. Yabe, New pretreatment systems using membrane separation technology, Desalination 98 (1994) 59–69.
[178] R.G. Chapman, E. Ostuni, M.N. Liang, G. Meluleni, E. Kim, L. Yan, G. Pier, H.S. Warren, G.M. Whitesides, Polymeric thin films that resist the adsorption of proteins and the adhesion of bacteria, Langmuir (2001) 1225–1233.
[179] A. Roosjen, H.J. Kaper, H.C. van der Mei, W. Norde, H.J. Busscher, Inhibition of adhesion of yeasts and bacteria by poly(ethylene oxide)-brushes on glass in a parallel plate flow chamber, Microbiology 149 (2003) 3239–3246.
[180] I. Cringus-Fundeanu, J. Luijten, H.C. van der Mei, H.J. Busscher, A.J. Schouten, Synthesis and characterization of surface-grafted polyacrylamide brushes and their inhibition of microbial adhesion, Langmuir (2007) 5120–5126.
[181] J.E. Raynor, T.A. Petrie, A.J. García, D.M. Collard, Controlling Cell Adhesion to titanium: functionalization of poly[oligo(ethylene glycol)methacrylate] brushes with cell-adhesive peptides, Adv. Mater. 19 (2007) 1724–1728.
[182] A.M. Brzozowska, E. Spruijt, A. de Keizer, M.A. Cohen Stuart, W. Norde, On the stability of the polymer brushes formed by adsorption of Ionomer complexes on hydrophilic and hydrophobic surfaces, J. Colloid Interface Sci. 353 (2011) 380–391.
[183] A.L. Ahmad, K.K. Lau, M.Z.A. Bakar, S.R.A. Shukor, Integrated CFD simulation of concentration polarization in narrow membrane channel, Comput. Chem. Eng. 29 (2005) 2087–2095.
[184] T. Icoz, Y. Jaluria, Design optimization of size and geometry of vortex promoter in a two-dimensional channel, J. Heat Transfer 128 (2006) 1081–1092.
[185] M. Amokrane, D. Sadaoui, M. Dudeck, C.P. Koutsou, New spacer designs for the performance improvement of the zigzag spacer configuration in spiral-wound membrane modules, Desalination Water Treat. 57 (2016) 5266–5274.
[186] A.L. Ahmad, K.K. Lau, Impact of different spacer filaments geometries on 2D unsteady hydrodynamics and concentration polarization in spiral wound membrane channel, J. Membr. Sci. 286 (2006) 77–92.
[187] A.I. Radu, M.S.H. van Steen, J.S. Vrouwenvelder, M.C.M. van Loosdrecht, C. Picioreanu, Spacer geometry and particle deposition in spiral wound membrane feed channels, Water Res. 64 (2014) 160–176.
[188] M. Fiebig, Vortex generators for compact heat exchangers, J. Enhanced Heat Transfer 2 (1995).
[189] G.A. Fimbres-Weihs, D.E. Wiley, Numerical study of mass transfer in three-dimensional spacer-filled narrow channels with steady flow, J. Membr. Sci. 306 (2007) 228–243.
[190] K. Majamaa, P.E.M. Aerts, C. Groot, L.r.L.M.J. Paping, W. van den Broek, S. van Agtmaal, Industrial water reuse with integrated membrane system increases the sustainability of the chemical manufacturing, Desalination Water Treat. (2010) 17–23.
[191] S.K. Karode, A. Kumar, Flow visualization through spacer filled channels by computational fluid dynamics I.: Pressure drop and shear rate calculations for flat sheet geometry, J. Membr. Sci. 193 (2001) 69–84.
[192] M. Amokrane, D. Sadaoui, M. Dudeck, Effect of inter-filament distance on the improvement of Reverse Osmosis desalination process, in: A.F.d.M. AFM (Ed.) AFM, Association Française de Mécanique, 2015, AFM, Association Française de Mécanique, Lyon, France (FR), 2015.